Universidade de Aveiro
2014

Departamento de Engenharia de Materiais
e Cerâmica

Diogo Pinto Cardoso Mirandela de Mendonça

Biosensors for the early diagnosis of Acute Myocardial Infarction

Universidade de Aveiro
2014

Departamento de Engenharia de Materiais e Cerâmica

Diogo Pinto Cardoso Mirandela de Mendonça

Biosensors for the early diagnosis of Acute Myocardial Infarction

Dissertação apresentada à Universidade de Aveiro para cumprimento dos requisitos necessários à obtenção do grau de Mestre em Materiais e Dispositivos Biomédicos, realizada sob a orientação científica da professora Doutora Paula Maria Lousada Silveirinha Vilarinho, Professora Associada com Agregação do Departamento de Engenharia de Materiais e Cerâmica da Universidade de Aveiro e co-orientação do professor Doutor Pedro Manuel Moreira da Rocha Vilarinho, Professor Auxiliar do Departamento de Economia, Gestão e Engenharia Industrial da Universidade de Aveiro e diretor do Acelerador de Comercialização de Tecnologias da COTEC-Portugal.

Aos meus pais, irmão, namorada e amigos por acreditarem nos meus devaneios e por me apoiarem na concretização dos meus sonhos.

o júri

presidente Prof. Doutor José Maria da Fonte Ferreira
Professor associado com agregação no Departamento de Engenharia de Materiais e Cerâmica

Prof. Doutor Fernando Manuel Tavares da Silva Ribeiro
Professor adjunto na Escola Superior de Saúde da Universidade de Aveiro

Prof.ª Doutora Paula Maria Lousada Silveirinha Vilarinho
Professora associada com agregação no Departamento de Engenharia de Materiais e Cerâmica

Agradecimentos

Gostaria de agradecer em primeiro lugar à professora Paula Vilarinho por me conceder a liberdade de trabalhar num projeto que tanto ambicionei. Quero agradecer as palavras de motivação e a forma entusiasta e dinamizadora com que sempre me orientou.

Ao professor Pedro Vilarinho o meu mais sincero obrigado por ter embarcado nos meus devaneios empreendedores. Foi um elemento fulcral quer no apoio ao desenvolvimento do projeto quer na transmissão de conhecimentos na área do empreendedorismo.

Deixo o meu mais profundo agradecimento ao professor Tito Trindade por me ter acolhido no seu grupo de investigação. Tem sido um privilégio fazer parte do seu grupo de trabalho e poder partilhar o seu laboratório com profissionais verdadeiramente talentosos e excecionais.

Aos colegas do *nanolab*, agradeço todo o apoio e acompanhamento. Agradeço em especial à Sara Fateixa pela ajuda, paciência e pelos conhecimentos que me transmitiu. Aprendi a conhecer um maravilhoso mundo novo na química, fora da minha área de conforto, e por isso vou estar-te sempre grato. Quando olho para trás vejo que aprendi imenso e a ti o devo. Não poderia deixar de agradecer ao Rui Silva e ao Rui Carvalho por todos os ensinamentos e pela forma como sempre se mostraram disponíveis em arranjar soluções para os problemas que ia encontrando ao longo do projeto.

Obrigado Rita Ramos por fazeres parte da minha vida e por me aturares nos bons e maus momentos. Obrigado por todos os momentos que me proporcionaste nesta efémera jornada académica.

Quero agradecer ao Tiago Adrega e ao Carlos Manta por terem abraçado este projeto. Tem sido um privilégio poder partilhar esta aventura empreendedora convosco.

Aos meus pais e irmão um mero agradecimento nunca será suficiente para exprimir a gratidão de toda uma vida, mas ainda assim pretendo fazê-lo neste formato. Obrigado por estarem sempre ao meu lado. Vocês são tudo para mim.

keywords

Acute Myocardial Infarction, cardiac troponin-I, biosensor, aptamers, SERS, metal nanoparticles

abstract

Acute Myocardial Infarction (AMI) is the leading cause of death and disability in industrialized countries and is expected to become so in emerging countries by 2020. AMI is one of the main diseases with the highest rate of misdiagnosis. Of the majority of patients that arrive to the Emergency Department (ED) with cardiac pain and other symptoms suggestive of myocardial infarction, only a small portion actually may experience an Acute Myocardial Infarction. Therefore, diagnosing Acute Myocardial Infarction within such a large proportion of patients with cardiac pain is indeed a diagnostic challenge.

For the correct diagnosis, it is essential to collect blood samples from the patient for the measurement of cardiac biomarkers, namely cardiac troponin I and cardiac troponin T.

In this thesis, it is proposed a new type of biosensor for the early and reliable diagnosis of Acute Myocardial Infarction based on the use of metallic nanoparticles attached with aptamers as new Surface Enhanced Raman Scattering (SERS) platforms for the specific detection of cardiac troponin-I. Firstly, gold and silver colloidal nanoparticles (NPs) were synthesized via the classical citrate reduction method and later characterized to assess the quality of the substrate. Larger gold nanoparticles (AuNPs) with sizes ranging from 35-96 nm were also prepared by a seed-mediated growth method. The detection of cardiac troponin I proceeded with the addition of the protein at lower concentrations to the metallic colloids. The final results showed that AuNPs with larger sizes are good candidates to be used as SERS platforms for the detection of cardiac troponin I, because they have presented the highest enhancement of the Raman signals of the protein. These experiments have shown that larger AuNPs are definitely most suitable for this kind of applications. Peak bands were found to be attributed from characteristic bands present in proteins.

Palavras-chave

Enfarte Agudo do Miocárdio, troponina cardíaca-I, biossensores, aptâmeros, SERS, nanopartículas metálicas

Resumo

O Enfarte Agudo do Miocárdio é a principal causa de morte e de incapacidade nos países desenvolvidos e prevê-se que seja também nos países em desenvolvimento até 2020. O Enfarte Agudo do Miocárdio é uma das principais patologias com a maior taxa de erro no diagnóstico. Entre a maioria de pacientes que se apresenta com dor torácica ou outro sintoma sugestivo de Enfarte Agudo do Miocárdio, apenas uma pequena porção de pacientes realmente manifesta a patologia. Deste modo, diagnosticar um Enfarte Agudo do Miocárdio numa larga proporção de pacientes com dor torácica é de facto um desafio para os clínicos.

Para o correto diagnóstico é essencial que se colete uma amostra de sangue do paciente para a medição de biomarcadores cardíacos sobretudo as troponinas cardíacas I e T.

Nesta tese propõe-se um novo tipo de biossensor para o diagnóstico precoce e fiável de Enfarte Agudo do Miocárdio que se baseia na funcionalização de aptâmeros à superfície de nanopartículas metálicas como novas plataformas de SERS (Surface Enhanced Raman Scattering) para a deteção específica da troponina cardíaca I. Numa primeira fase, nanopartículas de ouro e de prata foram sintetizadas pela via clássica de redução com citrato e subsequentemente caracterizadas para determinar a qualidade dos substratos obtidos.

Nanopartículas com tamanhos que rondam os 35-96 nm foram igualmente sintetizadas pelo processo de crescimento mediado por sementes. A deteção da troponina cardíaca I passou pela adição de baixas concentrações de proteína aos coloides metálicos. Os resultados finais demonstraram que as nanopartículas de ouro com tamanhos superiores aparentam ser bons candidatos a substratos para SERS para a deteção da troponina cardíaca-I, uma vez que apresentaram melhor intensificação de sinais de Raman da proteína. Estes testes permitiram concluir que as nanopartículas de ouro de maiores dimensões são de facto mais adequadas para este tipo de aplicações. Os picos obtidos podem ser atribuídos a bandas características encontradas nas proteínas.

Index

Figures

Tables

List of abbreviations

ACC – American College of Cardiology

ACS – Acute Coronary Syndrome

AgNPs – Silver Nanoparticles

AHA – American Heart Association

AMI – Acute Myocardial Infarction

AuNPs – Gold Nanoparticles

CAD – Coronary Artery Disease

CK – Creatine Kinase

CM – Chemical Mechanism

cTn – Cardiac troponins

cTnI – Cardiac troponin I

cTnT – Cardiac troponin T

CV – Coefficient of Variation

CVD – Cardiovascular Disease

ECG – Electrocardiogram

ED – Emergency Department

ELISA – Enzyme-linked Immunosorbent Assay

EM – Electromagnetic Mechanism

ESC – European Society of Cardiology

FTIR – Fourier Transform Infra-Red Analysis

LDL – Low-Density Lipoprotein

MS – Mass Spectrometry

MWCO – Molecular Weight Cut-Off

NACB – National Academy of Clinical Biochemistry

NPs –Nanoparticles

NSTE-ACS – Non-ST-segment Elevation ACS

PCR – Polymerase Chain Reaction

PEG – Polyethylene Glycol

PMA – Polymethacrylicacid

PMMA - Polymethylmethacrylate

PVA – Polyvinylalcohol

PVP - Polyvinylpyrrolidone

SELEX – Evolution of Ligands by Exponential Enrichment

SERS – Surface Enhanced Raman Scattering

SiNPs – Silica Nanoparticles

SM – Single Molecule

SPR – Surface Plasmon Resonance

STEM – Scanning Transmission Electron Microscopy

STEMI – ST-segment Elevation Myocardial Infraction

TBA – Thrombin Binding Aptamer

TEM – Transmission Electron Microscopy

UA – Unstable Angina

XRD – X-Ray Diffraction

Chapter 1

Introduction

1. Introduction

1.1. Structure of the thesis

This thesis is divided into five main chapters. The first chapter makes the bridge between problem-need-solution. In this chapter, the pathophysiology of Acute Myocardial Infarction and the way it is diagnosed in the clinical practice are reviewed in order to provide a better understanding of the real problem. After needs identification, it is presented a description of the proposed biosensor as an innovative solution for the early and reliable diagnosis of Acute Myocardial Infarction.

The second chapter is objectively targeted to the experimental synthesis and characterization of metallic nanoparticles, namely gold and silver, the chosen materials that will form the biosensor.

The third chapter presents the results of the detection of cardiac troponin I obtained by SERS analysis as a role model for the envisaged biosensor.

The fourth chapter summarizes the main conclusions of the attained results and states improvements and suggestions that will be implemented to the biosensor in the near future.

The fifth chapter is focused on the experimental procedures and instrumentation that were relevant to the proposed work. In this chapter, there is room for more experimental details, including a description of the functional principles of the employed instrumentation.

1.2. Overview of Acute Myocardial Infarction

Cardiovascular disease (CVD) is currently the leading cause of death and disability in industrialized countries and is expected to become so in emerging countries by 2020 [1, 2]. More than 17 million people died from CVDs in 2008. About 7.2 million of these deaths are due to coronary artery disease (CAD), also known as ischemic heart disease [1, 3-5].

Ischemic heart disease is a multi-factorial condition, resulting from the convergence of genetics, environment, diet and lifestyle. Recognized risk factors for the development of ischemic heart disease include family history, high blood pressure, smoking, elevated low-density lipoprotein (LDL cholesterol) diabetes, physical inactivity, and obesity. One of the main underlying pathological processes of ischemic heart disease is known as atherosclerosis [3, 6]. Atherosclerosis is an inflammatory process affecting medium and large sized blood vessels throughout the cardiovascular system. The process begins when LDL cholesterol, white blood cells and hemodynamic forces are combined specially at sites of disturbed laminar flow, namely where the arteries branch, leading to the formation of an atherosclerotic plaque. The formation of the atherosclerotic plaque is responsible for the narrowing of the arteries, compromising seriously the blood supply to the highly active cardiac muscle, the myocardium [6-9].

Plaque disruption is considered to occur as a result of the physical shear forces acting on it from inside the lumen or secondary to inflammatory and degradation processes within the plaque. In either case, the acute plaque disruption leads to a complex interaction between lipids, white blood cells and smooth-muscle cells exposed from the lipid core to the circulation, triggering the formation of a blood clot (thrombus) [10, 11].The blood clot may occlude the coronary blood vessels and interrupt coronary blood flow, resulting in Acute Myocardial Infarction (AMI). AMI compromises the blood supply to the myocardium, deprives the heart of oxygen and nutrients (ischemia) and leads to significant cardiac tissue destruction (cell death or necrosis) (Figure 1) [11-13].

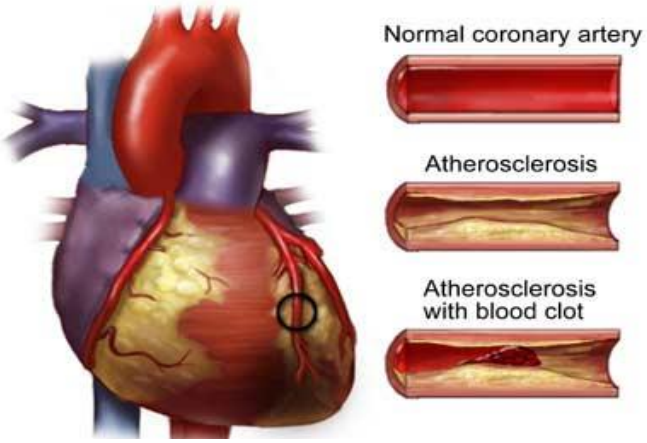

Figure 1. The underlying mechanisms of AMI [13].

The pathology is also characterized by a high rate of misdiagnosis since some true AMI patients are inappropriately discharged from hospitals, leading to an increase in the morbidity and mortality rates, while other non-AMI patients are unnecessary admitted to hospitals [14]. Approximately 15-20 million patients per year in the United States and Europe arrive to the Emergency Department (ED) with chest pain or other symptoms suggestive of AMI. However, it is known that only 10-15% of the patients with chest pain actually have myocardial infarction [15, 16].

Therefore, differentiating patients with symptoms suggestive of AMI within the very large proportion of patients with suspected cardiac pain is a diagnostic challenge, mainly in patients without clear symptoms or electrocardiographic features [1]. Since the majority of patients presenting with acute chest pain do not have acute ischemia, the rapid identification of these patients would substantially reduce both overcrowding of emergency departments and the costs with prolonged stays and unnecessary hospital admissions, estimated in billions of euros annually [16, 17]. Thus, an early and reliable diagnosis is extremely important, not only in saving lives but also in saving a great deal of time and costs in patient related care [14].

1.3. Pathophysiology of Acute Coronary Syndromes

The vast array of clinical symptoms manifested after coronary plaque disruption are often referred to as Acute Coronary Syndromes (ACS). ACS ranges from unstable angina (reversible myocardial injury) to myocardial infarction with large areas of irreversible damage (cardiac necrosis) [18, 19]. As shown in figure 2, ACS is mainly divided into two categories based on changes in electrocardiogram presentation: ST-segment elevation myocardial infarction (STEMI) characterized by a fully occluded coronary artery and non-ST-segment elevation ACS (NSTE-ACS) characterized by a partial or intermittently occluded coronary artery [18, 20-22].

NSTE-ACS (more frequent) is also sub-categorized in unstable angina (UA) and non-STEMI. Both possess similar pathogenesis and clinical presentations. However, ischemia in non-STEMI is more severe in intensity and duration and causes irreversible myocardial damage. Thus, it is crucial to accurately categorize patients prior to treatment [1, 23].

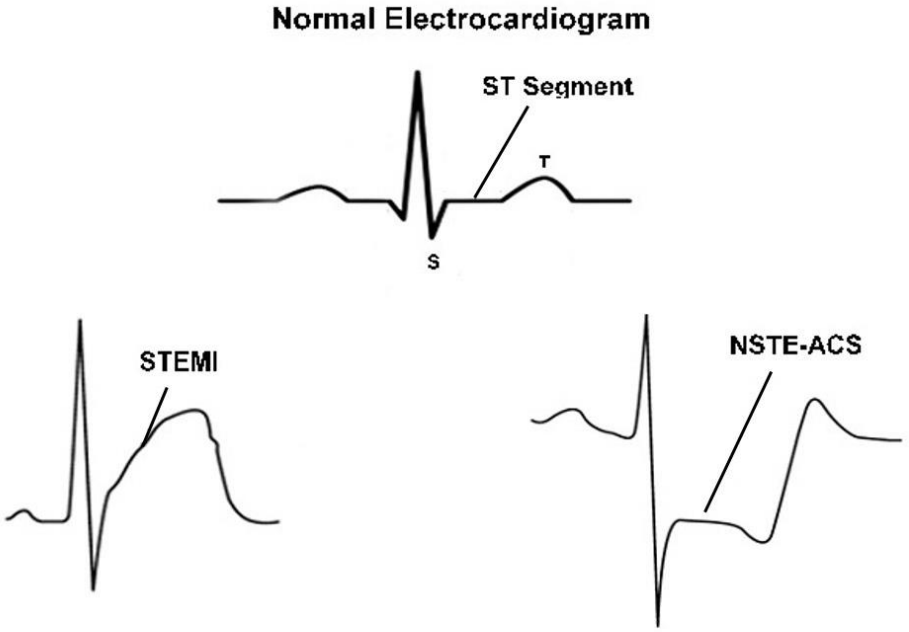

Figure 2. Categories of ACS based on electrocardiogram findings: STEMI and NSTE-ACS (NSTEMI/UA). Adapted from [22].

1.4. Diagnostic approach of Acute Myocardial Infarction

AMI is essentially diagnosed by clinical symptoms, electrocardiogram (ECG) findings and elevated values of biochemical markers (biomarkers) of myocardial necrosis in the blood [24]. The diagnosis of AMI is indeed a truly challenging task. Symptoms include chest discomfort but also discomfort in other areas of the upper body, shortness of breath, sweating, nausea, vomiting and dizziness. However, a lot of these symptoms are not specific of myocardial ischemia. In addition, symptoms of AMI in critically ill patients may be masked by sedative or analgesic medications; these patients are also frequently unable to communicate ischemic symptoms because of endotracheal intubation or coma [25].

The ECG is the initial clinical test for diagnosing myocardial ischemia and infarction. ECG changes that occur in association with acute ischemia and infarction include peaking of the T waves, ST-segment elevation and/or depression, changes in QRS complex and inversion of the T waves. The evolution of AMI and the formation of AMI electrocardiographic characteristic waves are illustrated in Figure 3 [26-28].

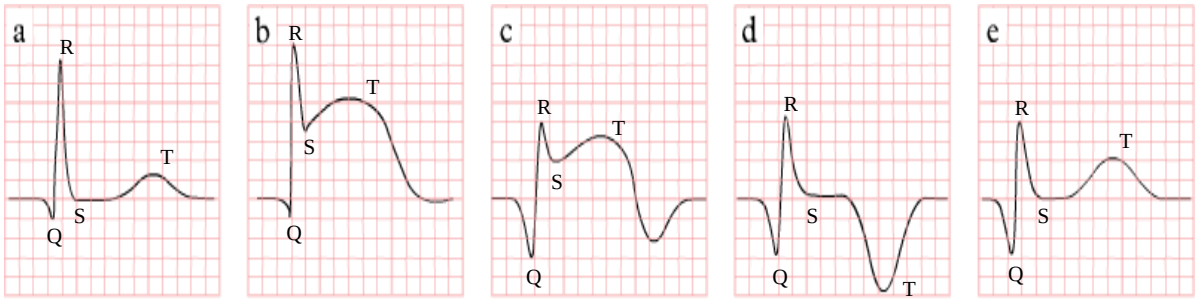

Figure 3. Evolution of AMI on the ECG. a) Normal, b) ST- segment elevation, c) Q wave formation d) T wave inversion, e) normalization with a persistent Q wave. Adapted from [28] .

The earliest manifestations of myocardial ischemia are typically T wave and ST-segment changes. In most patients with ST-elevation Myocardial Infarction (STEMI), clinical assessment and the ECG provide a straightforward diagnosis and allow the initiation of the proper treatment within minutes (Figure 4) [1, 16, 29]. Still, ECG alone is insufficient to diagnose AMI for two reasons: first, because ST segment deviation is observed in many other conditions [27]. Second, the diagnostic sensitivity of the initial ECG is about 50% for detecting myocardial damage, which means that many patients with AMI do not present significant ECG changes [30, 31].

Thus, It is mandatory to collect biochemical markers from the blood for the accurate assessment of myocardial necrosis because symptoms and ECG findings may be insufficient to diagnose AMI [18, 32, 33].

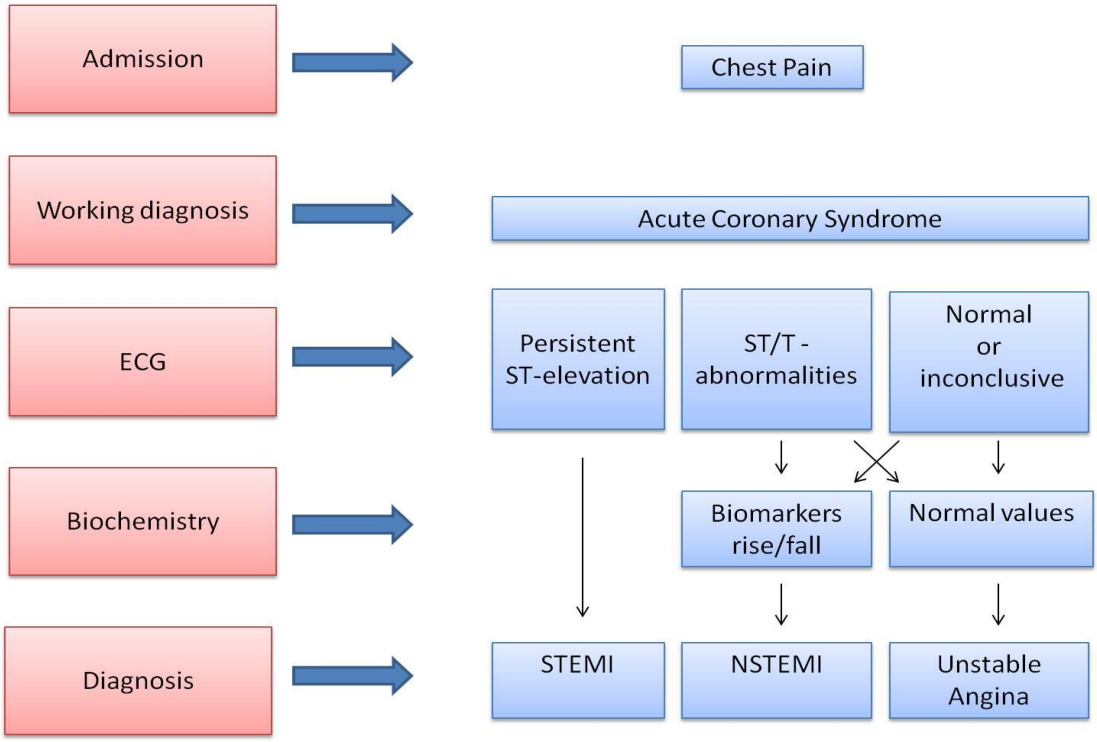

Figure 4. Diagnostic approach of ACS. When there is no ST-segment elevation on the ECG, the diagnosis of AMI relies on biochemical markers of necrosis. When there is a rise/fall of the biochemical markers an AMI or non-STEMI (NSTEMI) is present otherwise it is Unstable Angina. Adapted from [1].

1.5. Biomarker evaluation

A biomarker can be defined as a parameter that is objectively measured and evaluated as an indicator of normal biological processes, pathogenic processes or pharmacologic responses to a therapeutic intervention. A biomarker may be measured on a biosample (as blood, urine, or tissue test); it may be also a recording obtained from a person (blood pressure, Electrocardiogram) or even an imaging test (echocardiogram or CT scan) [34].

Cardiac biomarkers are protein components of cell structures that are released into the bloodstream when myocardial injury occurs. They play an important role in the diagnosis, risk stratification and treatment of patients with chest pain and suspected acute

coronary syndrome. The ideal characteristics for biomarkers of cardiac necrosis are summarized in table 1. [32]

Table 1. Ideal characteristics of Cardiac Necrosis Biomarkers [32].

• **Absolute cardiac specificity:** Biomarkers should not be present in non-cardiac tissues under any physiological or pathological conditions.
• **Specific for irreversible injury:** Biomarkers should differentiate ischemia from irreversible injury or necrosis.
• **Early release:** Biomarkers should be released shortly after necrosis.
• **High tissue sensitivity:** Biomarkers should be abundant in cardiac tissue and absent in blood under all pathological conditions except necrosis.
• **Stable release:** Biomarkers should persist in circulation for hours to days, following the acute necrotic event.
• **Estimate of infarct size:** Release of biomarkers should be in direct proportion to the extent of necrosis.
• **Measurable by conventional methods:** Biomarkers should allow quantitative measurement by reliable, rapid, precise and cost-effective methodology that is readily available.

Although several biomarkers satisfy one or more of these criteria, no single marker has yet been identified that satisfies them all [32]. The current gold-standard biomarker for the detection of myocardial necrosis are cardiac troponins (cTn), mainly cardiac troponin I (cTnI) and cardiac troponin T (cTnT) which have nearly absolute myocardial tissue specificity as well as high clinical sensitivity [35-37]. Several international scientific organizations such as the European Society of Cardiology (ESC), the American College of Cardiology (ACC), the American Heart Association (AHA), and the National Academy of Clinical Biochemistry (NACB) have recommended the use of these biomarkers when implementing new diagnostic strategies [18].

Troponin is an important protein of the thin filament (actin) of striated muscle and it is a complex of 3 subunits: C, T and I. Troponin T and I isoforms from the heart are structurally different from the corresponding forms found in skeletal muscle. The

measurement of cardiac troponin T and I isoforms is higher than other serum biomarkers of cardiac disease such as creatine kinase (CK) and myoglobin because they are also released in patients with skeletal muscle disease or injury [38, 39].

According to the last definition of AMI from the ESC, AHA and ACC, the detection of a rise and/or fall of cTn values is pivotal to the diagnosis of AMI [36, 40]. An increased value for cardiac troponin is defined as a measurement exceeding the 99th percentile of a normal reference population. The 99th percentile represents the decision level for the diagnosis of AMI and must be determined for each specific assay with appropriate quality control. [36, 40-43].

1.6. Market needs

Traditional technologies for molecular diagnostics such as Enzyme-Linked Immunosorbent Assay (ELISA), Mass Spectrometry (MS) and Polymerase Chain Reaction (PCR) are typically limited to laboratory facilities, rely on sample purification, expensive cutting-edge instruments, and labour intensive procedures [44]. Furthermore, some of these technologies still lack the sensitivity for detecting trace levels of biomarkers and require long and tedious assay time. In most recent technologies, circulating levels of troponin still may not become detectable for up to 3 to 4 hours (Figure 5) [45].

The ultrasensitive detection of cardiac biomarkers is fundamental for AMI diagnosis since many important biomarkers are present at ultra-low concentrations, especially during the early stage of AMI. [24] Increases in sensitivity of troponin assays will undoubtedly lessen the number of potentially AMI missed or delayed diagnosis, thus decreasing mortality and morbidity rates and costs related with the actual burden of the disease [36, 46].

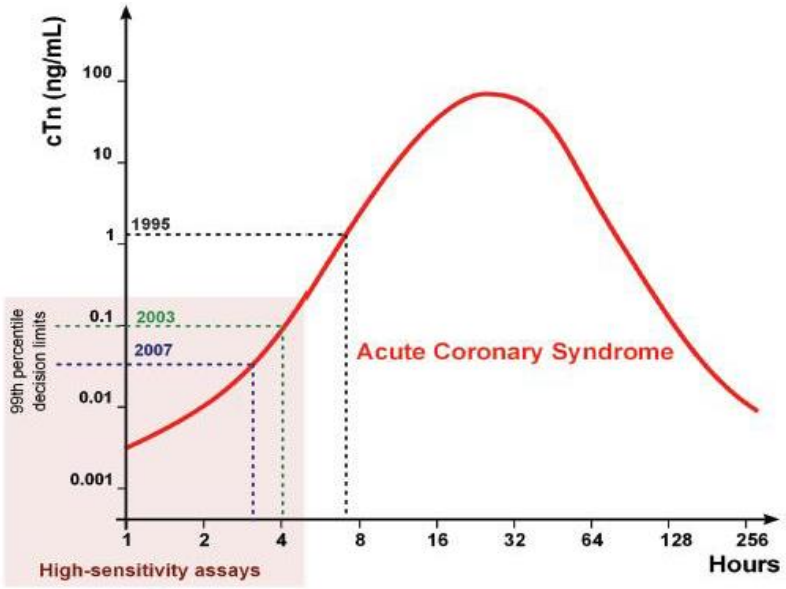

Figure 5. Evolution of cardiac troponin (cTn) assays and their diagnostic cutoffs [49].

However, for the development of more sensitive assays, one should not only consider the increase in sensitivity but also in precision, because increases in sensitivity come inevitably with a decrease in specificity, resulting in more false-positive results. For instance, the replacement of a sensitive troponin assay (Siemens Healthcare Diagnostics) for a more sensitive one in the Bringham and Women's Hospital Clinical Laboratories in early 2007 resulted in a doubling of positive troponin results in samples collected in the emergency department [45].

Increases in specificity are also important for the reliable exclusion of the disease in frequent dubious clinical settings. As a result, clinical uncertainties and unnecessary costs with overcrowding of emergency departments would be reduced with more straightforward diagnostic acuity. Accordingly, the use of a single biomarker may be insufficient to accurately categorize patients with acute coronary syndromes. Thus, the introduction of techniques that allow for the detection of multiple analytes simultaneously (multiplexing) may satisfy this constantly new growing need. Along with more diagnostic accuracy, multiplexing technologies enable lower sample consumptions, shorten turnaround times (time that goes from blood draw to test results reporting) and are more affordable in comparison with single-measurement assays [47-49].

Recently, different biosensor platforms have been designed with potential for the detection of available cardiac biomarkers [50]. In comparison with laboratory-based large instruments, biosensing devices are generally rapid, sensitive, selective and user-friendly and do not require tedious pre-treatment of samples [51, 52].

1.7. Biosensors

The concept of biosensor was proposed in the 80s [53]. Today there are more than 60 commercial devices available for about 120 different analytes. Among these are sensors for low molecular-mass substances, sensors for enzyme components and sensors for macromolecules. The current challenge is to design simple, inexpensive, accurate, sensitive and reliable biosensor platforms.

A biosensor can be defined as an analytical device comprising three basic components: i) a target recognition unit used to capture the specific target ii) a transducer that converts biorecognition events into quantifiable signals, iii) and a signal processing system that converts the signal into a readable form (Figure 6) [54-58].

The target recognition elements can be any chemical or biological components such as small organic molecules, proteins, antibodies, nucleic acids, carbohydrates, biological tissue and organelles [59-64]. The transducer system converts the biochemical reaction from the binding event into a physically detectable signal and can be divided into electrochemical, optical, piezoelectric, thermometric, ion-sensitive, magnetic or acoustic [55, 56, 59, 65].

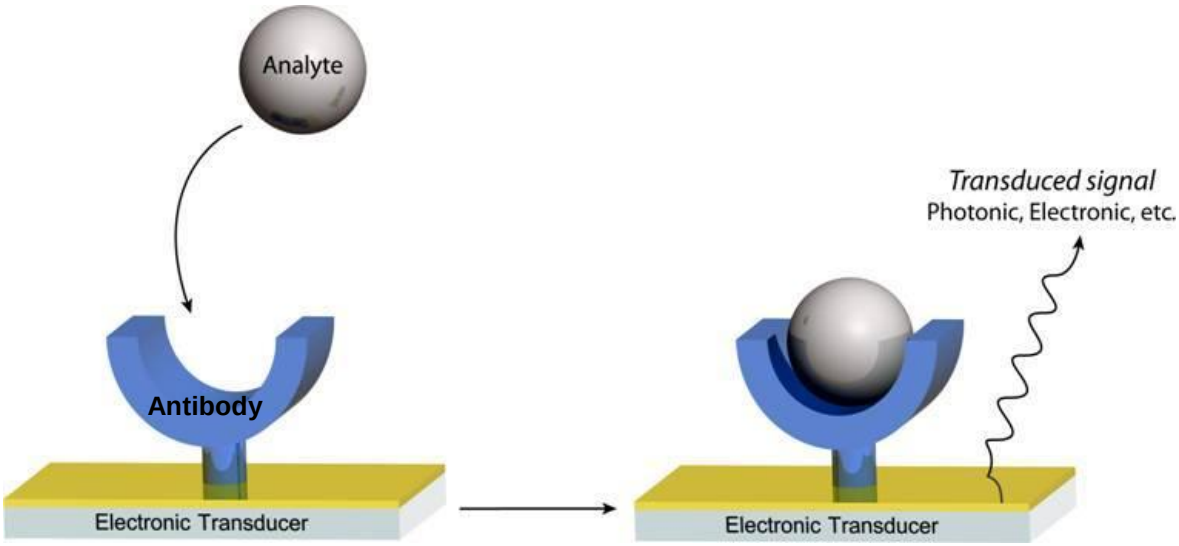

Figure 6. Principle of Biosensors. First, there is a biorecognition event with the molecules of interest. The biorecognition event is then converted into a quantifiable signal (electric, optic, piezoelectric, etc) which is finally processed into a readable form [58].

The sensitivity of the biosensor for the target analyte is greatly influenced by the transducer, whereas the selectivity is mainly dependent on the recognition element [51]. The ideal biosensor not only has to respond to low-concentrations of analytes, but also must have the ability to discriminate among species according to the recognition molecules that

are immobilized on its surface [66]. Table 2 describes commonly used methods for bionsensing platforms [67].

Table 2. Currently employed methods for biosensing platforms: Electrochemical (widely seen in glucose monitors), mechanical and optical formats. Adapted from [67].

Method	Mechanism	Features
Electrochemical	Detection of changes in electrical parameters at the active surface of electrodes that are proportional to the analyte concentration	**(+)** Real-time detection **(+)** Low-costs of fabrication **(+)** Widely employed (glucose monitors) **(-)** Limited sensitivities **(-)** Short shelf-life **(-)**Temperature, pH and ionic concentration dependency
Mechanical	Detection of changes in mass on the sensor surface due to the binding of biomolecules	**(+)** Label-free detection **(-)** Damping effects in liquid samples **(-)** Reduced sensitivity in liquids **(-)** Complex fabrication
Optical	Detection of variations in light intensity or refractive index changes	**(+)** Minimal sample preparation **(+)** Easy-to-use **(+)** Ultra-low sensitivities **(+)** Found in every laboratory **(-)** Costly opto-instrumentation **(-)** Set-up complexity

1.7.1 Nanomaterials as transducer elements

Nowadays it is well established that the performance of biosensors for the detection of biomolecules depends greatly on the influence of immobilization surfaces [68]. Among many immobilization surfaces, nanomaterials are being explored due to their exceptional optical and electrical properties, high surface-to-volume ratio, modified surface work function, high surface reaction activity, high catalytic efficiency and strong adsorption ability [69, 70].

Nanomaterial-based biosensors can achieve very low detection limits (even single molecule or cell) [71]. In addition they offer multi-detection possibilities and may ensure a high stability (more stable than enzymes or fluorescent dyes). Since nanomaterials have very high capacity for charge transfer they are likely to reach lower detection limits and higher sensitivity values. The microenvironment provided by a nanomaterial may help a biomolecule to retain its conformation with maximum biological activity [55, 70-72].

Metallic nanoparticles (NPs) such as gold (AuNPs) and silver (AgNPs) nanoparticles in particular, have attracted significant attention in the fields of biosensing and are preferably described in this thesis [73].

1.7.2 Metallic NPs

The unique physical and chemical properties of noble metal NPs have contributed to the development of new biosensing platforms with improved capabilities for the specific detection of bioanalytes [69]. Metallic NPs can be described as a lattice of ionic cores with conduction electrons moving almost freely inside [74]. Metallic NPs have an average size typically between 1 and 100 nm (100 to 1000 times smaller than human cells), which display unique optical properties different from those observed in the bulk materials [75].

When the size of the metallic NPs is reduced to a few nanometers, these optical properties are strongly enhanced due to what is called the Surface Plasmon Resonance (SPR) effect [76]. Basically, the phenomenon is characterized by a collective oscillation of the conduction electrons to the surface of the nanoparticle due to a “force” exerted by the electromagnetic field. As a consequence of the confinement of the electrons inside the nanoparticle, negative charge will be accumulated in one side and positive charge in the opposite one, creating an electric dipole. This dipole generates an electric field inside the nanoparticle, opposite to that of the light, compelling the electrons to return to the equilibrium position (Figure 7) [76-79].

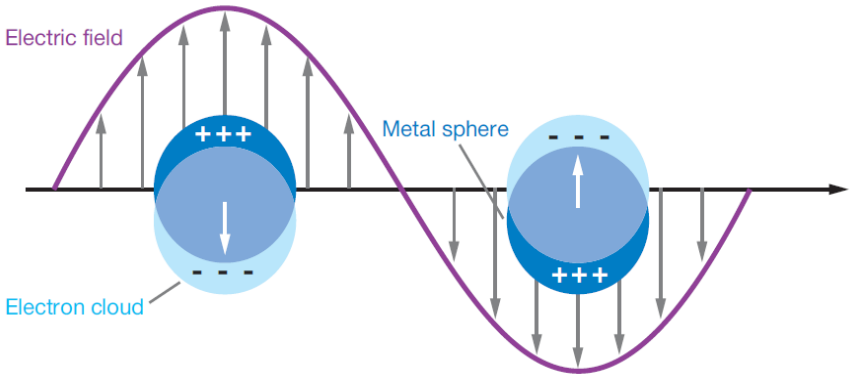

Figure 7. Illustration of the localized surface plasmon resonance effect and formation of an electric dipole [79].

In the particular case of AuNPs and AgNPs, the SPR effect yields exceptionally high absorption and scattering properties that allows them to have a higher sensitivity in optical detection methods than conventional organic dyes [69]. The SPR frequency is highly sensitive to the shape, size and composition of the nanoparticles, inter-particle distance and dielectric nature of its interface with the local environment, thus providing an effective way for tuning their optical properties (Figure 8) [79-84].

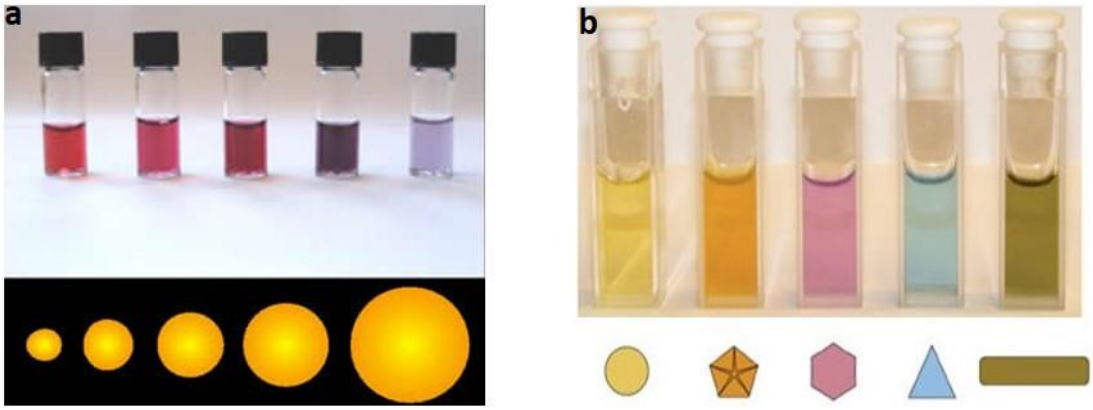

Figure 8. Modulating SPR properties of colloidal gold (a) and silver (b) solutions with variations in nanoparticle size and shape, respectively [83, 84].

The bright and distinct colours possessed by noble metal NPs are due to the SPR resulting from the collective oscillations of conduction band electrons excited by light of appropriate frequencies [85]. The Plasmon resonance property of AuNPs makes them most suitable engineered nanomaterials for bioimaging, biomedical therapeutics and biodiagnostic tools [86, 87]. For instance, biomolecule-conjugated AuNPs are largely used as biomarkers and biodelivery vehicles in medicine [88], pharmacy [89] and in cosmetic products [90]. What

makes AuNPs so desirable for medical applications over other metal nanoparticles is their inertness, less cytotoxicity, biocompatibility and also the easy surface modification with different biomolecules such as peptides, proteins and nucleic acids [70, 80, 91].

On the other hand, AgNPs have also attracted worldwide research interest due to their unique physical and chemical properties which lead to numerous potential applications in optical, electrical and biological industries [92]. For instance, they can be used as catalysts [93], sensors and biosensors [94], and antimicrobial agents [95].

AgNPs play a crucial role in inhibiting bacterial growth in aqueous and solid medium due to their high reactivity. The antibacterial properties of the silver-containing materials can be applied, for example, in medicine to reduce infections as well as to prevent bacteria colonization on medical instruments [96].

Silver exhibits the highest efficiency of plasmon excitation among the three metals (silver, gold and copper) that display SPR bands in the visible spectrum [97]. Moreover, optical excitation of plasmon resonances in AgNPs is the most efficient mechanism by which light interacts with matter. A single silver nanoparticle interacts with light more efficiently than a particle of the same dimension with any organic or inorganic chromophore. AgNPs capture much more light than is physically incident on them due to higher light-interaction cross-sections [97].

For these reasons, Au and Ag NPs were strategically chosen to be the transducer elements of the envisaged biosensor.

1.7.3 Synthesis of metallic NPs

Two complementary approaches have been known for the preparation of nanostructures: the first is the breakdown method (top-down) and the second is the build-up method (bottom-up) [98]. The top-down method typically uses advanced lithographic, milling and grinding technologies which reduce the dimensions of macro-scaled metals into smaller particles from the micrometer to the nanometer regimen followed by stabilization of the resulting nanosized metal particles by the addition of colloidal protecting agents [98, 99]. In the bottom up approach, smaller components of atomic or molecular dimensions self-assemble chemically to give rise to a larger and more organized system. Therefore, bottom-up strategies employ the chemical or electrochemical reduction of metal salts in solution (Figure 9) [100, 101].

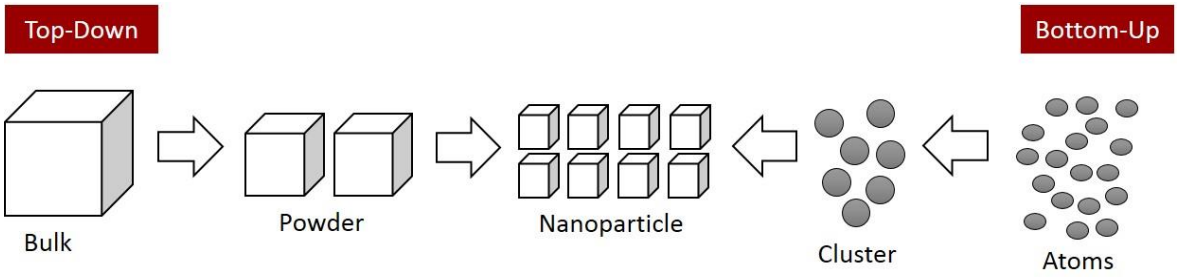

Figure 9. Illustration of the two complementary approaches for the preparation of nanostructures: Top-Down and Bottom-Up. Adapted from [101].

The chemical reduction method is one of the most used methods to prepare metallic NPs, in which metal salts are reduced to their metal states with reducing agents such as sodium citrate ($Na_3C_6H_5O_7$) and borohydride ($NaBH_4$) [102]. For instance, AuNPs are commonly prepared by the reduction of hydrogen tetrachloroaurate ($H[AuCl_4]$) with sodium citrate solution, wherein gold ions Au^{3+} are reduced to neutral gold atoms Au^0 [69, 103]. The citrate reduced Au colloidal solution has a red wine colour with an absorption in the visible region of approximately 520 nm [104]. This methods usually yields AuNPs in the 10–20 nm diameter range with relatively narrow size distributions [97].

On the other hand, AgNPs can be synthesized by following the methods used for AuNPs by replacing the gold salt with silver nitrate ($AgNO_3$) [75]. In this case, sodium citrates reduces silver ions (Ag^+) to metallic silver (Ag^0).The citrate reduced Ag colloidal solution has a yellow colour with an absorption maximum in the visible region of 420 nm [75, 92]. AgNPs prepared by the citrate reduction are nearly spherical and the crystallites have relatively large diameters (50–100 nm) and wide range distributions in size and shape [105, 106].

The advantages of the chemical reduction method include the facile fabrication of particles of various shapes along with narrow size distributions, the use of non-complicated equipment or instruments and the yield of large quantities of NPs in short time at low costs [107]. Moreover, it is possible to fine-tune the shape and size of the NPs by changing parameters such as the reducing agent, the reaction time and the temperature [107, 108].

In the process of chemical reduction, metal NPs require protective agents for stabilization and to prevent particles from sticking together by Van der Waals and electrostatic interactions (aggregation) in order to maintain its nanoscale properties. The two basic modes of stabilization which have been distinguished are electrostatic and steric. Electrostatic stabilization is based on the electrical double layer repulsion between the particles. (Figure 10) [109, 110]. Typically, the layer of adsorbed citrate anions at the surface

of AuNPs and AgNPs prevents aggregation due to electrostatic repulsion, keeping particles away from each other [111]. Therefore, sodium citrate acts both as a reducing and a stabilizer agent [108].

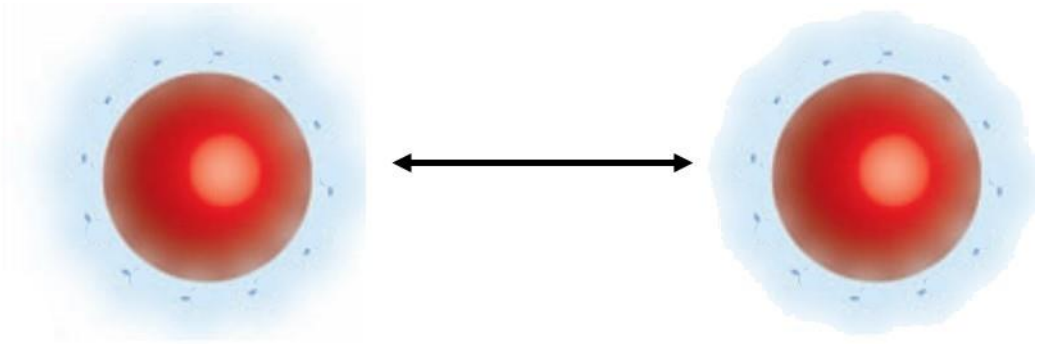

Figure 10. Electrostatic repulsion. Particles in suspension that possess, in this case, negative charges at the surface will tend to repel each other and there will be no tendency to form aggregates. Adapted from [110].

Another stabilization mechanism is based on the steric repulsion between molecules or ions adsorbed on neighbouring particles. [112]. Typically, long chains of organic molecules are used to provide a particular effective stabilization by acting as protective shields on the metallic surface. Thus, NPs are separated from each other and aggregation is prevented (Figure 11) [109, 113]. Size and chemical nature of these molecules determine the degree of stabilization. Polymeric compounds such as polyvinylalcohol (PVA), polyvinylpyrrolidone (PVP), polyethyleneglycol (PEG), polymethacrylicacid (PMA), and polymethylmethacrylate (PMMA) for instance are prime candidates for steric stabilization of nanoparticles [113, 114].

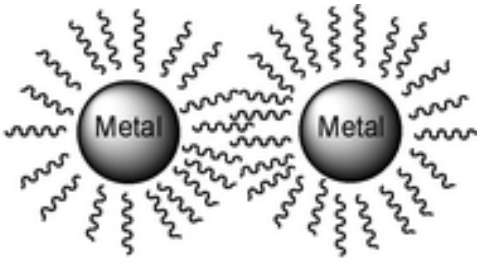

Figure 11. Steric stabilization. Long polymer chains and the arrangement of conical geometries on metal surfaces provide effective steric stabilization. Adapted from [109].

1.7.4 Aptamers as biorecognition elements

The specific detection of cardiac troponin I can be achieved with the incorporation of aptamers as biorecognition elements for the proposed biosensor. The term “aptamers” results from the combination of two words: “*aptus*” (meaning to fit) and the Greek word “*mers*” (particle) [115, 116]. Aptamers are small single-stranded molecules of RNA or DNA (oligonucleotides) that bind with extremely high specificity to various molecular targets such as small molecules, proteins, nucleic acids, cells or microorganisms [117, 118]. They are isolated and chemically synthesized *in vitro* from huge combinatorial libraries by a process known as Evolution of Ligands by Exponential Enrichment (SELEX) [57, 119].

The selection process starts when random sequences of 10^{14}-10^{15} oligonucleotide strands are chemically synthesized and amplified with Polymerase Chain Reaction (Figure 12). The nucleic acid library is incubated with a target molecule, often immobilized onto a solid state matrix such as gel or a column, so that the DNA or RNA which has affinity to the target molecule can be captured. The nucleic acids that bind to the target are then separated from the unbound strands and eluted from the target molecule for a new stage of amplification via PCR. After each round of selection there will be a new library of nucleic acid molecules containing more affinity to the target. The next rounds of selection are usually performed under more stringent conditions such as lower concentration of the target and shorter time for binding. Finally, the oligonucleotide that has higher affinity to its target molecule is obtained approximately after 10-20 cycles of the selection process [57, 120-124].

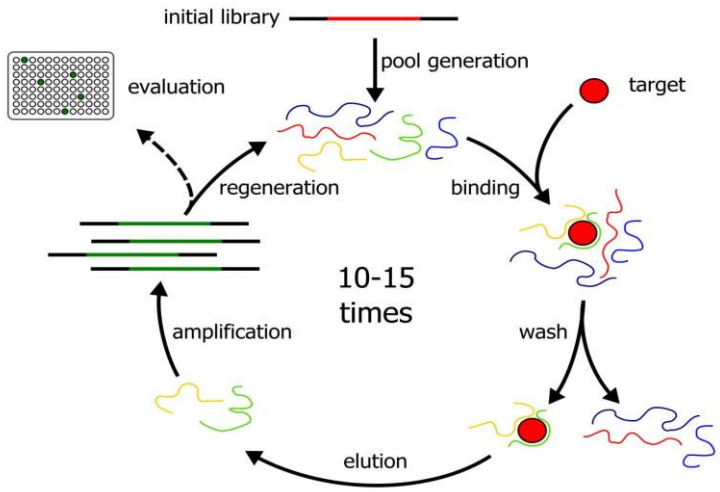

Figure 12. In the first step random DNA or RNA oligonucleotides and the target are incubated for binding. Unbound oligonucleotides are removed by several washing steps. The target-bound oligonucleotides are eluted and subsequently amplified by PCR [124].

The combination of metallic NPs with aptamers represents an incredible breakthrough innovation since there is nothing like it in the market. All the processes known in the market are based on immunoassays in which antibodies are targeted to cardiac biomarkers [125]. The problem with antibodies is that they are more expensive, need stringent storage and handling conditions and often require animals and cell cultures to be produced [126, 127]. Aptamers, on the contrary, exhibit several unique features in comparison with natural receptors such as enzymes and antibodies which include:

- **Binding efficiency**: Aptamers with higher affinity and specificity can be selected *in vitro* for any given target, not only large molecules such as proteins and cells but also to small molecules such as nucleotides, organic dyes, amino acids and metal ions whereas antibodies are generally competent in binding to mostly larger molecules [116, 126].

- **Chemical stability**: It is well known that proteins easily undergo irreversible denaturation and so lose easily their tertiary structures at high temperatures. On the other hand, oligonucleotides are more thermally stable and maintain their structures over repeated cycles of denaturation/renaturation [128].

- **Production:** The identification and production of monoclonal antibodies are laborious and very expensive processes involving screening of a large number of colonies. The clinical commercial success of antibodies has led to the need for very large-scale production in mammalian cell culture. Aptamers in contrast, once selected can be obtained in large amounts through chemical synthesis with great accuracy and reproducibility. These chemical processes are more cost-effective than the production of antibodies [128].

- **Target-reaching efficiency:** Aptamers can penetrate tissues faster and more efficiently due to their significantly lower molecular weights (8-25 kDa aptamers versus ~150 kDa antibodies). Therefore, aptamers penetrate barriers and reach their target sites *in vivo* more efficiently than the larger-sized protein antibodies [129].

- **Immunogenicity:** Aptamers are virtually non-immunogenic *in vivo,* which means that, in principle, they are not recognized by the immune system. Antibodies, on the contrary, are highly immunogenic since they stimulate an immune response *in vivo* [129].

- **Flexibility:** It is easy to chemically modify aptamers with a variety of tags or functional groups such as primary amine (NH_2) and thiol (SH) groups on either 5' or 3' ends, on the bases or on the backbone of DNA [120, 130].

1.7.5 Functionalization of aptamers onto metal NPs

Functionalization of NPs is necessary for their stability, functionality and biocompatibility [70]. Commonly used functionalization strategies are based on the use of Polyethylene glycol (PEG), oligonucleotides, peptides, antibodies and similar molecules [131-134]. Functionalization of metallic NPs involves the use of bifunctional ligands in which a moiety (-SH, -NH_2, -COOH) is used for anchorage to the NPs while the other is directed to the outer-surface for specific interaction with biomolecules [104]. Bifunctional ligands containing SH or NH_2 groups at one of their ends are preferred because they are prone to form strong gold-sulphur (Au-S) and gold-nitrogen (Au-N) bonds at the surfaces of metallic NPs [70].

The ultimate goal in functionalization is to preserve the properties of both metallic NPs and the bound biological molecules, which means that biological molecules should be stable and able to retain its biorecognition properties and metal NPs should be able to retain its unique properties such as strong Plasmon absorption bands, light scattering, among others [135, 136].

The key step for any aptamer-based sensor design involves the immobilization of the aptamer to the surface of the sensor. Physical adsorption, based on ionic, hydrophobic and Van der Waals forces, is the simplest immobilization method since it does not require any nucleic acid modification. It consists in contacting the aptamer solution with the surface for a defined period of time followed by subsequently washing steps for the removal of any non-adsorbed biomolecules. However, physical adsorption suffers from biomolecule desorption from the surface due to weak and reversible binding [136, 137].

Another non-covalent easy way to functionalize and stabilize metallic nanoparticle-bioconjugates is through electrostatic interactions between the metallic NPs and the biological molecules. For instance, positively charged metallic NPs can bind by stable ionic interactions to negatively charged functional groups [135].

Likewise strong negative charge on the citrate-stabilized AuNPs surface provides opportunity for electrostatic interaction with positively charged amine groups (NH_2) of lysine residues of proteins adsorbed on the nanoparticle surface [135, 138, 139].

On the other hand, methods based on chemisorption or covalent linkages have been widely employed. For example, aptamers labeled with a thiol group at one end can be easily chemisorbed onto the surfaces of AuNPs [59] whereas amine-labeled aptamers can be easily adsorbed on the surface of carboxyl-modified silica nanoparticles (SiNPS) [122] Thiol-based aptamers are most commonly used to prepare functionalized AuNPs through strong Au-S bonding [59]. Advantages of using a direct Au-S bond to attach a receptor molecule include a rapid covalent reaction and a formation of a stable monolayer [140].

1.7.6 Optical biosensing techniques

Optical detection techniques are currently regarded as the most sensitive techniques, allowing sensitivities down to nanomolar-femtomolar (10^{-9}-10^{-15}) [24]. Optical biosensors can be classified into **colorimetric, fluorescence, luminescence and surface plasmon resonance** [67].

In **colorimetric** and **fluorescence**-based detection either target or biorecognition molecules are labeled with chromogenic/fluorescent tags such as dyes. The change in the intensity of the color/fluorescence signal indicates the presence of the target molecules and the interaction strength between target and biorecognition molecules [50, 141]. Fluorescence detection is the most commonly used optical technique for the detection of biomolecules because of its high sensitivity and low detection limits [142]. However, fluorescence suffers from laborious labeling processes that may also interfere with the function of the biomolecule [142]. The sensitivity of fluorescence detection is often compromised by background signals coming from autofluorescence of sample components. Quantitative analysis is also challenging since fluorescent dyes on each molecule cannot be precisely controlled. Additionally, fluorescent dyes are costly, have a limited shelf-life and are often dependent on pH [67, 141].

The **luminescence** methods are widely categorized into two types, namely **chemiluminescence** and **electroluminescence**. In chemiluminescence, target binding causes photochemical reactions, either directly or with the help of an enzyme label (Figure 13) [67, 143]. In electroluminescence, the luminescence signal is generated by an electron transfer reaction of a luminescent compound immobilized near the proximity of an electrode

surface [50]. These techniques have distinct advantages such as the absence of light sources, which contribute to minimize scattered light and luminescent impurities.
Yet, highly sensitive detectors are usually extra-demanded to analyze the emitted photons during chemiluminescent reactions. Thus, low-cost sensitive photodetectors are still needed for the adoption of luminescence-based biosensors [67].

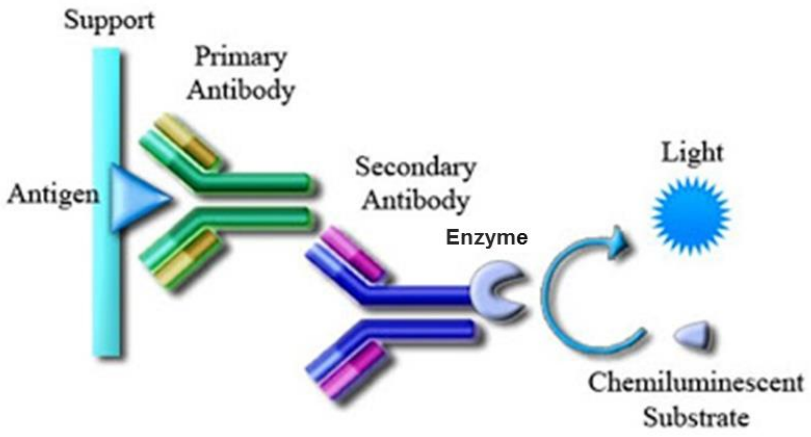

Figure 13. Illustration of a chemiluminescence method. The secondary antibody containing an enzyme label is conjugated to the primary antibody. A certain enzyme catalyzes the chemiluminescent substrate to produce light. Light is then measured with an external equipment called a luminometer [143].

Recently, **Surface Plasmon Resonance** (**SPR**) has become the preferred label-free optical method. When molecules with sufficient mass bind to the surface of noble metals, they disturb the plasmon and shift the resonance angle of an incident light. These shifts consist on minute refractive index changes on the surface and so can be used to detect the binding of mass to the surface (Figure 14) [144, 145]. While very powerful, the SPR technique relies solely on the ability of biomolecular recognition elements to recognize and capture target analytes. Therefore, the accuracy of SPR measurements can be compromised by interferences which produce a change in the refractive index but are not associated with the capture of the target. One source of interferences is non-specific interactions between the sensor surface and the sample, including adsorption of non-target molecules to the surface of the sensor and binding of structurally similar but not target molecules to the biomolecular biorecognition elements. Other interferences may occur for example from background refractive index changes such as sample temperature and composition fluctuations [142, 146, 147].

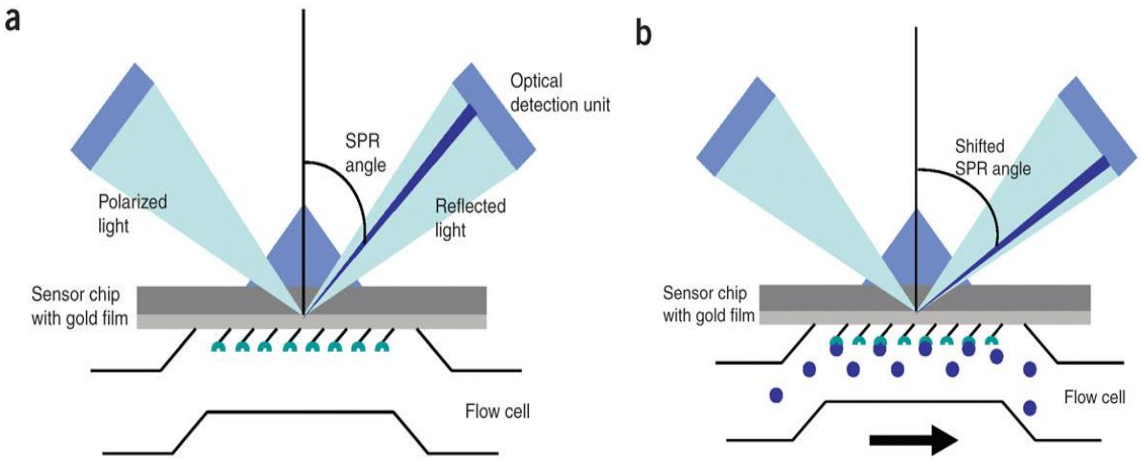

Figure 14. (a) A polarized light is applied to the surface of the sensor chip and is reflected. The intensity of the reflected light is adjusted to a certain incident angle, the SPR angle. (b) Interacting substances near the surface of the sensor chip increase the refractive index, which alters the SPR angle [145].

1.8. Surface enhanced Raman Scattering Spectroscopy

To address some of the limitations of current optical techniques Surface enhanced Raman Scattering spectroscopy (SERS) has recently awaken considerable interest for both *in vitro* and *in vivo* medical diagnostics [148-150]. SERS is an extension and variation of standard Raman Spectroscopy, a vibrational spectroscopic technique that provides detailed information about the interrogated substances at the molecular level [151].

Briefly, the Raman spectroscopic technique involves shining a laser source onto an unknown chemical sample. Most of the light that is absorbed by the sample will be scattered back at the same wavelength of the laser source. Thus, only a small portion of the light that is absorbed will be scattered at different wavelengths that are indicative of the vibrational transitions in the molecule. Since different molecules possess different vibrational modes, the spectrum of the inelastically scattered light can be thought as analogous to a molecular fingerprint. Despite this high specificity, traditional Raman Spectroscopy was considered limited because of the relatively weak signals and small scattering cross-sections [142, 152].

Nevertheless, this problem was mitigated with the advent of SERS in the late 1970s by showing that Raman signals could be enhanced by several orders of magnitude in the presence of nanostructered metal surfaces [148, 152-155]. This enhancement can be explained by two mechanisms: a) electromagnetic mechanism (EM) associated with large local fields caused by electromagnetic resonances occurring near metal surface structures and b) chemical mechanism (CM) involving a scattering process associated with chemical

interactions between the molecule and the metal surfaces. The electromagnetic mechanism is believed to contribute the most (10^4-10^7) to the observed intensity enhancement conversely to the chemical mechanism (10-10^2) [156, 157].

The huge local electromagnetic field enhancement is presumably from the so called Hot-Spots, spatially localized surface Plasmon resonances occurring between two or more closely spaced metal nanostructures [158]. It is believed that Hot-Spots are responsible for the single molecule (SM) sensitivity of SERS [159]. Nie's group [160] and Kneipp's group [161] have reported single molecule detection by SERS, indicating the high sensitivity of SERS for ultrasensitive chemical or biological detection. Moskovits's group has recently reported the detection of DNA by SERS based on EM Hot-Spots, further indicating the ability of SERS for the ultra-sensitive detection of biological molecules [162-164].

In addition to high sensitivity at single molecule, SERS offers the possibility for detection of multiple analytes at single excitation wavelengths because of the very narrow spectral widths of Raman peaks (typically 10-100 times narrower than fluorescence peaks) [148, 165, 166]. Nowadays there are two main SERS configurations for biosensing platforms: intrinsic or extrinsic [167]. In intrinsic detection, the analyte can be directly applied to the nanostructured surfaces and the Raman spectrum of the biomolecule directly measured to identify the specimen [151]. In extrinsic detection, antibodies, nucleic acids or related molecules can be immobilized onto metallic nanostructured surfaces in order to aid for capture and specific detection of the molecule of interest. (Figure 15) [151, 168].

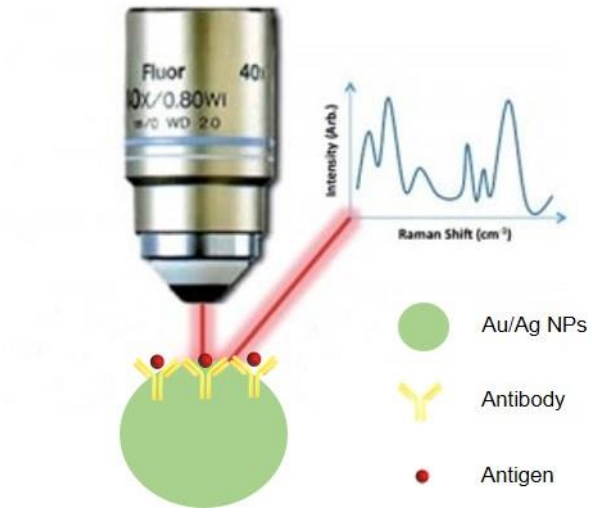

Figure 15. Extrinsic configuration of SERS for biosensing platforms. Adapted from [168].

The extrinsic SERS detection method with aptamers has been reported for the sensitive detection of thrombin (an enzyme involved in the coagulation process) [127, 162]. Based on the fact that thrombin can bind two Thrombin Binding Aptamers (TBA) at the same time, Wang *et al.,* reported an aptamer sandwich complex composed by TBA/ thrombin/ TBA-AuNPS as shown in Figure 16. [162] In this approach, the EM coupling effect was produced by Hot-Spots between AuNPs and AgNPs, where the Raman probes reside. Au substrate was bound to the 5' thiolated TBA and thrombin was then bound to the TBA through one of the active sites. AuNPS labeled by TBA and Raman probes were then bound to the thrombin immobilized on the Au substrate through the other binding site of thrombin. The detection limit of this SERS aptasensor was 5×10^{-10}M.

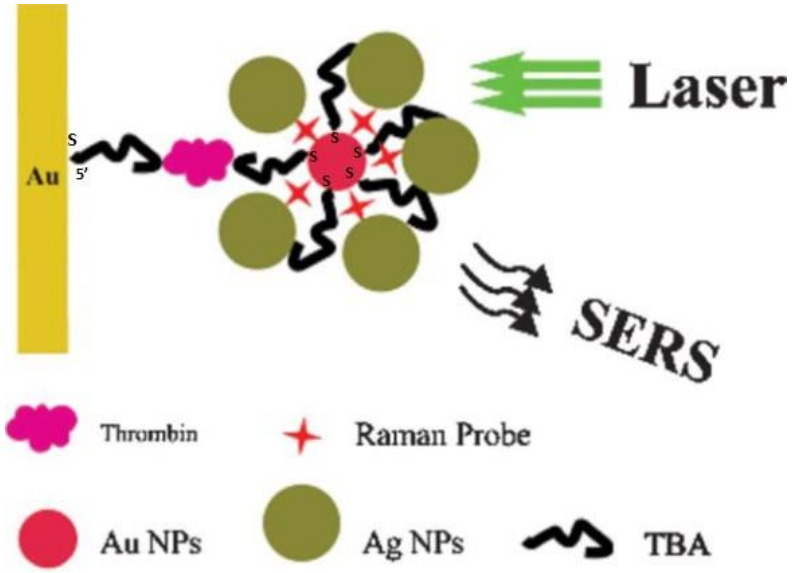

Figure 16. Schematic illustration of a SERS aptasensor for thrombin detection. TBA bounds to the Au substrate with a thiol group at the 5' end and leaves another active site for binding with thrombin. AuNPs labelled with TBA and Raman probes were then bound to the thrombin immobilized on the Au substrate through the other binding site of thrombin. AgNPs were employed to enhance the signal of the Raman probes due to the EM coupling effect between AuNPs and AgNPs. Adapted from [162]

1.9. Objectives

The first objective of this work is dedicated to the synthesis and characterization of metallic NPs with different sizes and nature (Au and Ag). This step is very important to select the optimal structural and morphological characteristics for the detection of human cardiac troponin I.

The second objective aims for the detection of human cardiac troponin I with an intrinsic SERS configuration. The idea is to simply apply the supplied cardiac troponin I at low concentration on the surface of Au and Ag NPs (for comparison) followed by a stringent analysis of the resulting spectrum. SERS can provide a lot of information about protein structure, orientation and environment that needs to be addressed and primarily understood since there is still much to know about cardiac troponin I.

1.10. References

[1] Hamm, C. W., Bassand, J. P., Agewall, S., Bax, J.*, et al.*, "ESC Guidelines for the management of acute coronary syndromes in patients presenting without persistent ST-segment elevation: The Task Force for the management of acute coronary syndromes (ACS) in patients presenting without persistent ST-segment elevation of the European Society of Cardiology (ESC)", *European Heart Journal,* vol. 32, pp. 2999-3054, 2011.

[2] Arrebola, M. M., Lillo, J. A., Diez De Los Rios, M. J., Rodriguez, M.*, et al.*, "Analytical performance of a sensitive assay for cardiac troponin I with loci technology", *Clin Biochemistry,* vol. 43, pp. 998-1002, 2010.

[3] "Global Atlas on Cardiovascular disease prevention and control " World Health Organization in collaboration with the World Heart Federation and the World Stroke Organization, 2011.

[4] Wallace, T. C., "Anthocyanins in cardiovascular disease," *Advances in Nutrition,* vol. 2, pp. 1-7, 2011.

[5] Yang, L., Kuper, H., and Weiderpass, E., "Anthropometric characteristics as predictors of coronary heart disease in women", *Journal of Internal Medicine,* vol. 264, pp. 39-49, 2008.

[6] Bhatia, S. K., *Biomaterials for clinical applications*, 2010.

[7] Schiener, M., Hossann, M., Viola, J. R., Ortega-Gomez, A.*, et al.*, "Nanomedicine-based strategies for treatment of atherosclerosis", *Trends in Molecular Medicine,* vol. 20, pp. 271-81, 2014.

[8] Fayad, Z. A. and Fuster, V., "Clinical Imaging of the High-Risk or Vulnerable Atherosclerotic Plaque", *Circulation Research,* vol. 89, pp. 305-316, 2001.

[9] Weber, C. and Noels, H., "Atherosclerosis: current pathogenesis and therapeutic options," *Nature Medicine,* vol. 17, pp. 1410-22, 2011.

[10] Wang, T., Palucci, D., Law, K., Yanagawa, B.*, et al.*, "Atherosclerosis: pathogenesis and pathology", *Diagnostic Histopathology,* vol. 18, pp. 461-467, 2012.

[11] Landesberg, G., "The pathophysiology of perioperative myocardial infarction: facts and perspectives", *Journal of Cardiothoracic and Vascular Anesthesia,* vol. 17, pp. 90-100, 2003.

[12] Pasotti, M., Prati, F., and Arbustini, E., "The pathology of myocardial infarction in the pre- and post-interventional era", *Heart,* vol. 92, pp. 1552-6, 2006.
[13] http://medicscientist.com/acute-myocardial-infarction-causes-pathophysiology-etiology (06-01-2014).
[14] Yang, Z. and Min Zhou, D., "Cardiac markers and their point-of-care testing for diagnosis of acute myocardial infarction", *Clinical Biochemistry,* vol. 39, pp. 771-80, 2006.
[15] Reichlin, T., Steuer, S., Biedert, S., Stelzig, C*., et al.*, "Early Diagnosis of Myocardial Infarction with Sensitive Cardiac Troponin Assays", *The new england journal of medicine,* 2009.
[16] Twerenbold, R., Jaffe, A., Reichlin, T., Reiter, M*., et al.*, "High-sensitive troponin T measurements: what do we gain and what are the challenges?", *European Heart Journal,* vol. 33, pp. 579-86, 2012.
[17] Zimmerman, J., Fromm, R., Meyer, D., Boudreaux, A*., et al.*, "Diagnostic Marker Cooperative Study for the Diagnosis of Myocardial Infarction", *Circulation,* vol. 99, pp. 1671-1677, 1999.
[18] McDonnell, B., Hearty, S., Leonard, P., and O'Kennedy, R., "Cardiac biomarkers and the case for point-of-care testing", *Clinical Biochemistry,* vol. 42, pp. 549-61, 2009.
[19] Daga, C. L., Kaul, U., and Mansoor, A., "Approach to STEMI and NSTEMI", *SUPPLEMENT TO JAPI,* vol. 59, 2011.
[20] Sheppard, L., "Acute coronary syndromes", *Continuing Education in Anaesthesia, Critical Care & Pain,* vol. 4, pp. 175-180, 2004.
[21] Nutescu, A. E., "Diagnosing Acute Coronary Syndrome and determining patient risk ", *Johns Hopkins Advanced Studies in Medicine,* vol. 6, 2006.
[22] http://www.learnonly.com/2011/12/types-of-heart-attack-stemi-myocardial.html (06-01-2014).
[23] Yiadom, M. Y., "Emergency department treatment of acute coronary syndromes," *Emergency Medicine Clinics of North America,* vol. 29, pp. 699-710, 2011.
[24] Hasanzadeh, M., Shadjou, N., Soleymani, J., Omidinia, E*., et al.*, "Optical immunosensing of effective cardiac biomarkers on acute myocardial infarction", *Trends in Analytical Chemistry,* vol. 51, pp. 158-168, 2013.
[25] Lim, W., Qushmaq, I., Cook, D. J., Crowther, M. A*., et al.*, "Elevated troponin and myocardial infarction in the intensive care unit: a prospective study", Journal of *Critical Care,* vol. 9, pp. R636-44, 2005.
[26] Wagner, G. S., Macfarlane, P., Wellens, H., Josephson, M*., et al.*, "AHA/ACCF/HRS recommendations for the standardization and interpretation of the electrocardiogram: part VI: acute ischemia/infarction: a scientific statement from the American Heart Association Electrocardiography and Arrhythmias Committee, Council on Clinical Cardiology; the American College of Cardiology Foundation; and the Heart Rhythm Society: endorsed by the International Society for Computerized Electrocardiology", *Circulation,* vol. 119, pp. e262-70, 2009.
[27] Herring, N. and Paterson, D. J., "ECG diagnosis of acute ischaemia and infarction: past, present and future", *QJM,* vol. 99, pp. 219-30, 2006.
[28] http://en.ecgpedia.org/wiki/File:AMI_evolutie.png (18-01-2014).
[29] Ahmad, M. I., "Biomarkers in Acute Myocardial Infarction", *Journal of Clinical & Experimental Cardiology,* vol. 03, pp. 1-8, 2012.
[30] Karimian, N., Vagin, M., Zavar, M. H., Chamsaz, M*., et al.*, "An ultrasensitive molecularly-imprinted human cardiac troponin sensor", *Biosensors and Bioelectronics,* vol. 50, pp. 492-8, 2013.
[31] Reiter, M., Reichlin, T., Twerenbold, R., and Mueller, C., "Diagnosis of Acute Myocardial Infarction using Highly Sensitive Cardiac Troponin Assays", 2011.

[32] Morrow, D. A., *Cardiovascular Biomarkers - Pathophysiology and Disease Management,* 2006.
[33] Hammarsten, O., "Small Changes in Cardiac Troponin Levels Are Common in Patients with Myocardial Infarction: Diagnostic Implications", *Conference Papers in Medicine,* vol. 2013, pp. 1-5, 2013.
[34] Vasan, R. S., "Biomarkers of cardiovascular disease: molecular basis and practical considerations", *Circulation,* vol. 113, pp. 2335-62, 2006.
[35] Keller, T., Zeller, T., Roth, A., Baldus, S.*, et al.*, "Sensitive Troponin I Assay in Early Diagnosis of Acute Myocardial Infarction", *The new england journal of medicine,* 2009.
[36] Thygesen, K., Alpert, J. S., Jaffe, A. S., Simoons, M. L.*, et al.*, "Third universal definition of myocardial infarction", *Journal of the American College of Cardiology,* vol. 60, pp. 1581-98, 2012.
[37] Apple, F. S., Smith, S. W., Pearce, L. A., Ler, R.*, et al.*, "Use of the bioMerieux VIDAS troponin I ultra assay for the diagnosis of myocardial infarction and detection of adverse events in patients presenting with symptoms suggestive of acute coronary syndrome", *Clinica Chimica Acta,* vol. 390, pp. 72-5, 2008.
[38] Wu, A. H., "Cardiac troponin: friend of the cardiac physician, foe to the cardiac patient?", *Circulation,* vol. 114, pp. 1673-5, 2006.
[39] A, C., W.K., C., Cheng, S. H., Leung, C. K.*, et al.*, "Troponin-I, myoglobin, and mass concentration of creatine kinase-MB in acute myocardial infarction", *QJM,* vol. 92, pp. 711-718, 1999.
[40] Thygesen, K., Alpert, J. S., White, H. D., "Universal definition of myocardial infarction", *European Heart Journal,* vol. 28, pp. 2525-38, 2007.
[41] Apple, F. S., "A new season for cardiac troponin assays: it's time to keep a scorecard", *Clinical Chemistry,* vol. 55, pp. 1303-6, 2009.
[42] Hamm, C. W., "Cardiac Troponin Elevations in Patients Without Acute Coronary Syndrome", *Circulation,* vol. 106, pp. 2871-2872, 2002.
[43] Thygesen, K., Mair, J., Giannitsis, E., Mueller, C.*, et al.*, "How to use high-sensitivity cardiac troponins in acute cardiac care", *European Heart Journal,* vol. 33, pp. 2252-7, 2012.
[44] Song, Y., Huang, Y. Y., Liu, X., Zhang, X.*, et al.*, "Point-of-care technologies for molecular diagnostics using a drop of blood", *Trends in Biotechnology,* vol. 32, pp. 132-9, 2014.
[45] Mahajan, V. S. and Jarolim, P., "How to interpret elevated cardiac troponin levels", *Circulation,* vol. 124, pp. 2350-4, 2011.
[46] Meune, C., Balmelli, C., Vogler, E., Twerenbold, R.*, et al.*, "Consideration of high-sensitivity troponin values below the 99th percentile at presentation: does it improve diagnostic accuracy?", *International Journal of Cardiology,* vol. 168, pp. 3752-7, 2013.
[47] Kuhn, E., Addona, T., Keshishian, H., Burgess, M.*, et al.*, "Developing multiplexed assays for troponin I and interleukin-33 in plasma by peptide immunoaffinity enrichment and targeted mass spectrometry", *Clinical Chemistry,* vol. 55, pp. 1108-17, 2009.
[48] Katus, H., Searle, J., and Giannitsis, E., "How to Use High-Sensitivity Cardiac Troponins in Acute Cardiac Care?", *Conference Papers in Medicine,* vol. 2013, pp. 1-4, 2013.
[49] Lea, P., Keystone, E., Mudumba, S., Kahama, A.*, et al.*, "Advantages of multiplex proteomics in clinical immunology: the case of rheumatoid arthritis: novel IgXPLEX: planar microarray diagnosis", *Clinical Revies in Allergy & Immunology,* vol. 41, pp. 20-35, 2011.

[50] Qureshi, A., Gurbuz, Y., and Niazi, J. H., "Biosensors for cardiac biomarkers detection: A review", *Sensors and Actuators B: Chemical,* vol. 171-172, pp. 62-76, 2012.
[51] Castillo, J., Gáspár, S., Leth, S., Niculescu, M.*, et al.*, "Biosensors for life quality", *Sensors and Actuators B: Chemical,* vol. 102, pp. 179-194, 2004.
[52] Ge, X., Asiri, A. M., Du, D., Wen, W.*, et al.*, "Nanomaterial-enhanced paper-based biosensors",*Trends in Analytical Chemistry,* vol. 58, pp. 31-39, 2014.
[53] Malhotra, B. D. and Turner, A. P., *Advances in Biosensors: Perspectives in Biosensors*, 2003.
[54] Yoo, E. H. and Lee, S. Y., "Glucose biosensors: an overview of use in clinical practice", *Sensors (Basel),* vol. 10, pp. 4558-76, 2010.
[55] Singh, R., Mukherjee, M. D., Sumana, G., Gupta, R. K.*, et al.*, "Biosensors for pathogen detection: A smart approach towards clinical diagnosis", *Sensors and Actuators B: Chemical,* vol. 197, pp. 385-404, 2014.
[56] Malhotra, B. D., Singhal, R., Chaubey, A., Sharma, S. K.*, et al.*, "Recent trends in biosensors", *Current Applied Physics,* vol. 5, pp. 92-97, 2005.
[57] Smuc, T., Ahn, I. Y., and Ulrich, H., "Nucleic acid aptamers as high affinity ligands in biotechnology and biosensorics", *Journal of Pharmaceutical and Biomedical Analysis,* vol. 81-82, pp. 210-7, 2013.
[58] https://weizmanngroup.uchicago.edu/page/dna-biosensors (12-06.2014).
[59] Chiu, T. C. and Huang, C. C., "Aptamer-functionalized nano-biosensors", *Sensors (Basel),* vol. 9, pp. 10356-88, 2009.
[60] Wang, P., Xu, G., Qin, L., Xu, Y.*, et al.*, "Cell-based biosensors and its application in biomedicine", *Sensors and Actuators B: Chemical,* vol. 108, pp. 576-584, 2005.
[61] Perumal, V. and Hashim, U., "Advances in biosensors: Principle, architecture and applications", *Journal of Applied Biomedicine,* vol. 12, pp. 1-15, 2014.
[62] Omidfar, K., Khorsand, F., and Darziani Azizi, M., "New analytical applications of gold nanoparticles as label in antibody based sensors", *Biosensors and Bioelectronics,* vol. 43, pp. 336-47, 2013.
[63] Sassolas, A., Blum, L. J., and Leca-Bouvier, B. D., "Optical detection systems using immobilized aptamers", *Biosensors and Bioelectronics,* vol. 26, pp. 3725-36, 2011.
[64] Abbasian, S., Moshaii, A., Nikkhah, M., and Farkhari, N., "Adsorption of DNA on colloidal Ag nanoparticles: effects of nanoparticle surface charge, base content and length of DNA", *Colloids and Surfaces B: Biointerfaces,* vol. 116, pp. 439-45, 2014.
[65] Monošík, R., Streďanský, M., and Šturdík, E., "Biosensors - classification, characterization and new trends", *Acta Chimica Slovaca,* vol. 5, 2012.
[66] Leung, A., Shankar, P. M., and Mutharasan, R., "A review of fiber-optic biosensors", *Sensors and Actuators B: Chemical,* vol. 125, pp. 688-703, 2007.
[67] Pires, N. M., Dong, T., Hanke, U., and Hoivik, N., "Recent developments in optical detection technologies in lab-on-a-chip devices for biosensing applications", *Sensors (Basel),* vol. 14, pp. 15458-79, 2014.
[68] Pingarrón, J. M., Yáñez-Sedeño, P., and González-Cortés, A., "Gold nanoparticle-based electrochemical biosensors", *Electrochimica Acta,* vol. 53, pp. 5848-5866, 2008.
[69] Doria, G., Conde, J., Veigas, B., Giestas, L.*, et al.*, "Noble metal nanoparticles for biosensing applications", *Sensors (Basel),* vol. 12, pp. 1657-87, 2012.
[70] Tiwari, P., Vig, K., Dennis, V., and Singh, S., "Functionalized Gold Nanoparticles and Their Biomedical Applications", *Nanomaterials,* vol. 1, pp. 31-63, 2011.
[71] Pérez-López, B. and Merkoçi, A., "Nanomaterials based biosensors for food analysis applications", *Trends in Food Science & Technology,* vol. 22, pp. 625-639, 2011.
[72] Cao, X., Ye, Y., and Liu, S., "Gold nanoparticle-based signal amplification for biosensing", *Analytical Biochemistry,* vol. 417, pp. 1-16, 2011.

[73] Sanvicens, N., Pastells, C., Pascual, N., and Marco, M. P., "Nanoparticle-based biosensors for detection of pathogenic bacteria",*Trends in Analytical Chemistry,* vol. 28, pp. 1243-1252, 2009.
[74] Cao, J., Sun, T., and Grattan, K. T. V., "Gold nanorod-based localized surface plasmon resonance biosensors: A review", *Sensors and Actuators B: Chemical,* vol. 195, pp. 332-351, 2014.
[75] Reddy, V. R., Currao, A., and Calzaferri, G., "Gold and silver metal nanoparticle-modified AgCl photocatalyst for water oxidation to O2", *Journal of Physics: Conference Series,* vol. 61, pp. 960-965, 2007.
[76] Garcia, M. A., "Surface plasmons in metallic nanoparticles: fundamentals and applications", *Journal of Physics D: Applied Physics,* vol. 44, p. 283001, 2011.
[77] Petryayeva, E. and Krull, U. J., "Localized surface plasmon resonance: nanostructures, bioassays and biosensing--a review", *Analytica ChimicaActa,* vol. 706, pp. 8-24, 2011.
[78] Stiles, P. L., Dieringer, J. A., Shah, N. C., and Van Duyne, R. P., "Surface-enhanced Raman spectroscopy", *Annual Reviews of Analytical Chemistry,* vol. 1, pp. 601-26, 2008.
[79] Willets, K. A. and Van Duyne, R. P., "Localized surface plasmon resonance spectroscopy and sensing", *Annual Reviews of Physical Chemistry,* vol. 58, pp. 267-97, 2007.
[80] Khan, M. S., Vishakante, G. D., and Siddaramaiah, H., "Gold nanoparticles: a paradigm shift in biomedical applications", *Advances in Colloid and Interface Science,* vol. 199-200, pp. 44-58, 2013.
[81] Zhao, J., Zhang, X., Yonzon, C. R., Haes, A. J.*, et al.*, "Localized Surface Plasmon Resonance Biosensors ", *Nanomedicine,* 2006.
[82] Tabor, C. E., "Some optical and catalytic properties of metallic nanoparticles ", Georgia Institute of Technology, 2009.
[83] http://www.photonics.com/Article.aspx?AID=41849 (20-05-2014).
[84] http://pure.rhul.ac.uk/portal/en/persons/mikhail-soloviev(2b06f036-2cc0-4375-87e1-57f662534d0d).html (20-05-2014).
[85] Howes, P. D., Rana, S., and Stevens, M. M., "Plasmonic nanomaterials for biodiagnostics", *Chemical Society Reviews,* vol. 43, pp. 3835-53, 2014.
[86] Hu, R., Zhang, X.-B., Kong, R.-M., Zhao, X.-H.*, et al.*, "Nucleic acid-functionalized nanomaterials for bioimaging applications", *Journal of Materials Chemistry,* vol. 21, p. 16323, 2011.
[87] Lim, E. K., Jang, E., Lee, K., Haam, S.*, et al.*, "Delivery of cancer therapeutics using nanotechnology", *Pharmaceutics,* vol. 5, pp. 294-317, 2013.
[88] Ghosh, P., Han, G., De, M., Kim, C. K.*, et al.*, "Gold nanoparticles in delivery applications," *Advanced Drug Delivery Reviews,* vol. 60, pp. 1307-15, 2008.
[89] Chandra, P., Singh, J., Singh, A., Srivastava, A.*, et al.*, "Gold Nanoparticles and Nanocomposites in Clinical Diagnostics Using Electrochemical Methods", *Journal of Nanoparticles,* vol. 2013, pp. 1-12, 2013.
[90] Verma, H. N., Singh, P., and Chavan, R. M., "Gold nanoparticle: synthesis and characterization", *Veterinary World,* vol. 7, pp. 72-77, 2014.
[91] Di Pasqua, A. J., Mishler, R. E., Ship, Y.-L., Dabrowiak, J. C.*, et al.*, "Preparation of antibody-conjugated gold nanoparticles", *Materials Letters,* vol. 63, pp. 1876-1879, 2009.
[92] Li, H. and Xu, D., "Silver nanoparticles as labels for applications in bioassays", *Trends in Analytical Chemistry,* vol. 61, pp. 67-73, 2014.
[93] Tran, Q. H., Nguyen, V. Q., and Le, A.-T., "Silver nanoparticles: synthesis, properties, toxicology, applications and perspectives", *Advances in Natural Sciences: Nanoscience and Nanotechnology,* vol. 4, p. 033001, 2013.

[94] Ren, X., Meng, X., Chen, D., Tang, F.*, et al.*, "Using silver nanoparticle to enhance current response of biosensor", *Biosensors and Bioelectronics,* vol. 21, pp. 433-7, 2005.
[95] Abdel-Aziz, M. S., Shaheen, M. S., El-Nekeety, A. A., and Abdel-Wahhab, M. A., "Antioxidant and antibacterial activity of silver nanoparticles biosynthesized using Chenopodium murale leaf extract", *Journal of Saudi Chemical Society,* vol. 18, pp. 356-363, 2014.
[96] Guzmán, M. G., Dille, J., and Godet, S., "Synthesis of silver nanoparticles by chemical reduction method and their antibacterial activity", vol. 2, pp. 315-322, 2008.
[97] Evanoff, D. D., Jr. and Chumanov, G., "Synthesis and optical properties of silver nanoparticles and arrays", *Chemphyschem,* vol. 6, pp. 1221-31, 2005.
[98] Pelton, M. and Bryant, G., *Introduction to metal-nanoparticle plasmonics,* 2013.
[99] Hulteen, J. C., Treichel, D. A., Smith, M. T., Duval, M. L.*, et al.*, "Nanosphere Lithography: Size-Tunable Silver Nanoparticle and Surface Cluster Arrays", *The Journal of Physical Chemistry B,* vol. 103, pp. 3854-3863, 1999.
[100] Merza, K. S., "Comparative Study on Methods for Preparation of Gold Nanoparticles", *Green and Sustainable Chemistry,* vol. 02, pp. 26-28, 2012.
[101] http://nanotechnologie-medecine.webnode.fr/les-nanotechnologie-une-technologie-de-pointe-/la-fabrication-des-nanotechnologie/ (03-07-2014).
[102] Akbarzadeh, A., Zare, D., Farhangi, A., Mehrabi, M. R.*, et al.*, "Synthesis and Characterization of Gold Nanoparticles by Tryptophane", *American Journal of Applied sciences,* vol. 6, pp. 691-695, 2009.
[103] Zhao, P., Li, N., and Astruc, D., "State of the art in gold nanoparticle synthesis", *Coordination Chemistry Reviews,* vol. 257, pp. 638-665, 2013.
[104] Baptista, P., Pereira, E., Eaton, P., Doria, G.*, et al.*, "Gold nanoparticles for the development of clinical diagnosis methods," *Analytical and Bioanalytical Chemistry,* vol. 391, pp. 943-50, 2008.
[105] Pillai, Z. S. and Kamat, P. V., "What Factors Control the Size and Shape of Silver Nanoparticles in the Citrate Ion Reduction Method?", *Journal of Physical Chemistry B,* vol. 108, pp. 945-951, 2004.
[106] Zhang, W., Qiao, X., and Chen, J., "Synthesis of silver nanoparticles—Effects of concerned parameters in water/oil microemulsion", *Materials Science and Engineering: B,* vol. 142, pp. 1-15, 2007.
[107] Horikoshi, S. and Serpone, N., *Microwaves in nanoparticle synthesis*, 2013.
[108] Hussain, J. I., "Silver nanoparticles: preparation, characterization, and kinetics", *Advanced Materials Letters,* vol. 2, pp. 188-194, 2011.
[109] Zhou, J., Ralston, J., Sedev, R., and Beattie, D. A., "Functionalized gold nanoparticles: synthesis, structure and colloid stability", *Journal of Colloid and Interface Science,* vol. 331, pp. 251-62, 2009.
[110] Azzazy, H. M., Mansour, M. M., Samir, T. M., and Franco, R., "Gold nanoparticles in the clinical laboratory: principles of preparation and applications", *Clinical Chemistry and Laboratory Medicine,* vol. 50, pp. 193-209, 2012.
[111] Mykola, M., Alexandre, R., Mykhaylo, L., and Alexey, S., "Experimental Approach Using Covalently Attached Fluorophore for Quantification of Oligonucleotide Immobilization on Gold Nanoparticles", *Colloids and Interface Science Communications,* vol. 1, pp. 35-38, 2014.
[112] Bajpai, S. K., Mohan, Y. M., Bajpai, M., Tankhiwale, R.*, et al.*, "Synthesis of Polymer Stabilized Silver and Gold Nanostructures", *Journal of Nanoscience and Nanotechnology,* vol. 7, pp. 2994-3010, 2007.
[113] Balanta, A., Godard, C., and Claver, C., "Pd nanoparticles for C-C coupling reactions", *Chemical Society Reviews,* vol. 40, pp. 4973-85, 2011.
[114] Texter, J., *Reactions and synthesis in surfactant systems*, 2005.

[115] Wang, W., Chen, C., Qian, M., and Zhao, X. S., "Aptamer biosensor for protein detection using gold nanoparticles", *Analytical Biochemistry,* 2008.
[116] Aquino-Jarquin, G. and Toscano-Garibay, J. D., "RNA Aptamer Evolution: Two Decades of SELEction", *International Journal of Molecular Science,* 2011.
[117] Sosic, A., Meneghello, A., Cretaio, E., and Gatto, B., "Human Thrombin Detection Through a Sandwich Aptamer Microarray: Interaction Analysis in Solution and in Solid Phase", vol.11, pp. 9426-9441, 2011.
[118] Yuan, Q., Lu, D., Zhang, X., Chen, Z*., et al.*, "Aptamer-conjugated optical nanomaterials for bioanalysis", *Trends in Analytical Chemistry,* vol. 39, pp. 72-86, 2012.
[119] Yang, L., Zhang, X., Ye, M., Jiang, J*., et al.*, "Aptamer-conjugated nanomaterials and their applications", *Advanced Drug Delivery Reviews,* vol. 63, pp. 1361-1370, 2011.
[120] Lee, J. H., Higit, M. V., Mazumdar, D., and Lu, Y., "Molecular diagnostic and drug delivery agents based on aptamer-nanomaterial conjugates", *Advanced Drug Delivery Reviews,* vol. 62, pp. 592-605, 2010.
[121] Radom, F., Jurek, P. M., Mazurek, M. P., Otlewski, J*., et al.*, "Aptamers: Molecules of great potential", *Biotechnology Advances,*vol. 31, pp. 1260-1274, 2013.
[122] Wang, G., Wang, Y., Chen, L., and Choo, J., "Nanomaterial-assisted aptamers for optical sensing", *Biosensors and Bioelectronics,* vol. 25, pp. 1859-68, 2010.
[123] Stoltenburg, R., Reinemann, C., and Strehlitz, B., "SELEX--a (r)evolutionary method to generate high-affinity nucleic acid ligands", *Biomolecular Engineering,* vol. 24, pp. 381-403, 2007.
[124] http://www.chem-station.com/chemglossary/2014/03/-selex.html (15-07-2014).
[125] Ng, A. H., Uddayasankar, U., and Wheeler, A. R., "Immunoassays in microfluidic systems", *Analytical and Bioanalytical Chemistry,* vol. 397, pp. 991-1007, 2010.
[126] Cheng, A. K., Sen, D., and Yu, H. Z., "Design and testing of aptamer-based electrochemical biosensors for proteins and small molecules", *Bioelectrochemistry,* vol. 77, pp. 1-12, 2009.
[127] Yoon, J., Choi, N., Ko, J., Kim, K*., et al.*, "Highly sensitive detection of thrombin using SERS-based magnetic aptasensors", *Biosensors and Bioelectronics,* vol. 47, pp. 62-7, 2013.
[128] Song, K. M., Lee, S., and Ban, C., "Aptamers and their biological applications", *Sensors (Basel),* vol. 12, pp. 612-31, 2012.
[129] Sun, H., Zhu, X., Lu, P. Y., Rosato, R. R*., et al.*, "Oligonucleotide aptamers: new tools for targeted cancer therapy", *Molecular Therapy - Nucleic Acids,* vol. 3, p. e182, 2014.
[130] Kashefi-Kheyrabadi, L. and Mehrgardi, M. A., "Aptamer-conjugated silver nanoparticles for electrochemical detection of adenosine triphosphate", *Biosensors and Bioelectronics,* 2012.
[131] Guo, J., Gao, X., Su, L., Xia, H*., et al.*, "Aptamer-functionalized PEG-PLGA nanoparticles for enhanced anti-glioma drug delivery", *Biomaterials,* vol. 32, pp. 8010-20, 2011.
[132] Kumar, A., Ma, H., Zhang, X., Huang, K*., et al.*, "Gold nanoparticles functionalized with therapeutic and targeted peptides for cancer treatment", *Biomaterials,* vol. 33, pp. 1180-9, 2012.
[133] Raoof, M., Corr, S. J., Kaluarachchi, W. D., Massey, K. L*., et al.*, "Stability of antibody-conjugated gold nanoparticles in the endolysosomal nanoenvironment: implications for noninvasive radiofrequency-based cancer therapy", *Nanomedicine,* vol. 8, pp. 1096-105, 2012.
[134] Cordray, M. S., Amdahl, M., and Richards-Kortum, R. R., "Gold nanoparticle aggregation for quantification of oligonucleotides: optimization and increased dynamic range", *Analytical Biochemistry,* vol. 431, pp. 99-105, 2012.

[135] Delong, R. K., Reynolds, C. M., Malcolm, Y., Schaeffer, A.*, et al.*, "Functionalized gold nanoparticles for the binding, stabilization, and delivery of therapeutic DNA, RNA, and other biological macromolecules", Journal of *Nanotechnology, Science and Applications,* vol. 3, pp. 53-63, 2010.
[136] Sassolas, A., Blum, L. J., and Leca-Bouvier, B. D., "Optical detection systems using immobilized aptamers", *Biosensors and Bioelectronics,* 2011.
[137] Avvakumova, S., Colombo, M., Tortora, P., and Prosperi, D., "Biotechnological approaches toward nanoparticle biofunctionalization", *Trends in Biotechnology,* vol. 32, pp. 11-20, 2014.
[138] An, H. and Jin, B., "Prospects of nanoparticle-DNA binding and its implications in medical biotechnology", *Biotechnoly Advances,* vol. 30, pp. 1721-32, 2012.
[139] Ravindran, A., Chandran, P., and Khan, S. S., "Biofunctionalized silver nanoparticles: advances and prospects", *Colloids and Surfaces B: Biointerfaces,* vol. 105, pp. 342-52, 2013.
[140] Zhang, X. and Yadavalli, V. K., "Surface immobilization of DNA aptamers for biosensing and protein interaction analysis", *Biosensors and Bioelectronics,* vol. 26, pp. 3142-7, 2011.
[141] Fan, X., White, I. M., Shopova, S. I., Zhu, H.*, et al.*, "Sensitive optical biosensors for unlabeled targets: a review", *Analytica Chimica Acta,* vol. 620, pp. 8-26, 2008.
[142] Huh, Y. S., Chung, A. J., and Erickson, D., "Surface enhanced Raman spectroscopy and its application to molecular and cellular analysis", *Microfluidics and Nanofluidics,* vol. 6, pp. 285-297, 2009.
[143] http://medicalab.blogspot.pt/2012/08/trilogy-of-luminescence-part-iii.html (03-09-2014).
[144] Mitchell, J., "Small molecule immunosensing using surface plasmon resonance", *Sensors (Basel),* vol. 10, pp. 7323-46, 2010.
[145] Madeira, A., Ohman, E., Nilsson, A., Sjogren, B.*, et al.*, "Coupling surface plasmon resonance to mass spectrometry to discover novel protein-protein interactions", *Nature Protocols,* vol. 4, pp. 1023-1037, 2009.
[146] Yamamoto, M., Surface Plasmon Resonance (SPR) Theory: Tutorial, 2008.
[147] Narayanaswamy, R. and Wolfbeis, O. S., *Optical Sensors: Industrial, Environmental and Diagnostic Applications*, 2004.
[148] Wilson, A. J. and Willets, K. A., "Surface-enhanced Raman scattering imaging using noble metal nanoparticles", *Nanomedicine and Nanobiotechnology,* vol. 5, pp. 180-9, 2013.
[149] Huang, X. and El-Sayed, M. A., "Gold nanoparticles: Optical properties and implementations in cancer diagnosis and photothermal therapy", *Journal of Advanced Research,* vol. 1, pp. 13-28, 2010.
[150] Driscoll, A. J., Harpster, M. H., and Johnson, P. A., "The development of surface-enhanced Raman scattering as a detection modality for portable in vitro diagnostics: progress and challenges", *Physical Chemistry Chemical Physics,* vol. 15, pp. 20415-33, 2013.
[151] Tripp, R. A., Dluhy, R. A., and Zhao, Y., "Novel nanostructures for SERS biosensing", *Nano Today,* vol. 3, pp. 31-37, 2008.
[152] Delfino, I., Bizzarri, A. R., and Cannistraro, S., "Single-molecule detection of yeast cytochrome c by Surface-Enhanced Raman Spectroscopy", *Biophysical Chemistry,* vol. 113, pp. 41-51, 2005.
[153] Moskovits, M., "Enhanced Raman scattering by molecules adsorbed on electrodes--a theoretical model," *Solid State Communications,* vol. 32, pp. 59-62, 1979.
[154] Crookell, A., Fleischmann, M., Hanniet, M., and Hendra, P. J., "Surface-enhanced fourier transform raman spectroscopy in the near infrared", *Chemical Physics Letters,* vol. 149, pp. 123-127, 1988.

[155] Moskovits, M., "Surface roughness and the enhanced intensity of Raman scattering by molecules adsorbed on metals", *The Journal of Chemical Physics,* vol. 69, pp. 4159-4161, 1978.
[156] Vo-Tinh, T., "SERS chemical sensors and biosensors" new tools forenvironmental and biological analysis", *Sensors and Actuators B: Chemical,* 1995.
[157] Guillot, N. and de la Chapelle, M. L., "The electromagnetic effect in surface enhanced Raman scattering: Enhancement optimization using precisely controlled nanostructures", *Journal of Quantitative Spectroscopy and Radiative Transfer,* vol. 113, pp. 2321-2333, 2012.
[158] Shiohara, A., Wang, Y., and Liz-Marzán, L. M., "Recent approaches toward creation of hot spots for SERS detection", *Journal of Photochemistry and Photobiology C: Photochemistry Reviews,* 2014.
[159] Le Ru, E. C. and Etchegoin, P. G., "Sub-wavelength localization of hot-spots in SERS", *Chemical Physics Letters,* vol. 396, pp.393-397, 2004.
[160] Doering, W. E. and Nie, S., "Single-Molecule and Single-Nanoparticle SERS: Examining the Roles of Surface Active Sites and Chemical Enhancement", The *Journal of Physical Chemistry B,* vol. 106, pp. 311-317, 2002.
[161] Kneipp, K., Kneipp, H., and Kneipp, J., "Surface-Enhanced Raman Scattering in Local Optical Fields of Silver and Gold Nanoaggregates From Single-Molecule Raman Spectroscopy to Ultrasensitive Probing in Live Cells", *Accounts of Chemical Research.,* vol. 39, pp. 443-450, 2006.
[162] Wang, Y., Wei, H., Li, B., Ren, W.*, et al.*, "SERS opens a new way in aptasensor for protein recognition with high sensitivity and selectivity", *Chemical Communications,* pp. 5220-2, 2007.
[163] Suh, J. S. and Moskovits, M., "Surface-enhanced Raman spectroscopy of amino acids and nucleotide bases adsorbed on silver", *Journal of the American Chemical Society,* vol. 108, pp. 4711-4718, 1986.
[164] Moskovits, M., Braun, G., Lee, S. J., Dante, M.*, et al.*, "Surface-Enhanced Raman Spectroscopy for DNA Detection by Nanoparticle Assembly onto Smooth Metal Films", *Journal of the American. Chemical Society.,* vol. 129, pp. 6378-6379, 2007.
[165] Han, X. X., Ozaki, Y., and Zhao, B., "Label-free detection in biological applications of surface-enhanced Raman scattering",*Trends in Analytical Chemistry,* vol. 38, pp. 67-78, 2012.
[166] Vendrell, M., Maiti, K. K., Dhaliwal, K., and Chang, Y. T., "Surface-enhanced Raman scattering in cancer detection and imaging", *Trends in Biotechnology,* vol. 31, pp. 249-57, 2013.
[167] Guerrini, L. and Graham, D., "Molecularly-mediated assemblies of plasmonic nanoparticles for Surface-Enhanced Raman Spectroscopy applications", *Chemical Society Reviews,* vol. 41, pp. 7085-107, 2012.
[168] http://prospect.rsc.org/blogs/cw/2012/10/17/2p-or-not-2p-that-is-the-title/ (15-09-2014)

Chapter 2

Synthesis and characterization of metallic NPs

2. Synthesis and characterization of metallic NPs

2.1. Citrate reduction method

AuNPs were prepared by the reduction of hydrogen tetrachloroaurate ($H[AuCl_4]$) with sodium citrate solution, accordingly with the method first developed by Turkevich [1] and AgNPs were prepared by the reduction of silver nitrate ($AgNO_3$) also with sodium citrate solution.

For the characterization of the as-prepared metallic NPs, several techniques such as optical spectroscopy, vibrational spectroscopy, microscopy analysis and others were employed in order to have further evidence about their size, size distribution, shape and stability in aqueous solution.

Firstly, metallic NPs (Au and Ag) were characterized by optical measurements. The formation of Au and Ag NPs was followed by measuring the absorption of the solutions at wavelengths ranged from 300-800 nm. Figure 17 shows the optical spectra of the metallic NPs, where absorption bands at 428 and 520 nm, characteristic of the SPR band of AgNPs and AuNPs, respectively can be observed.

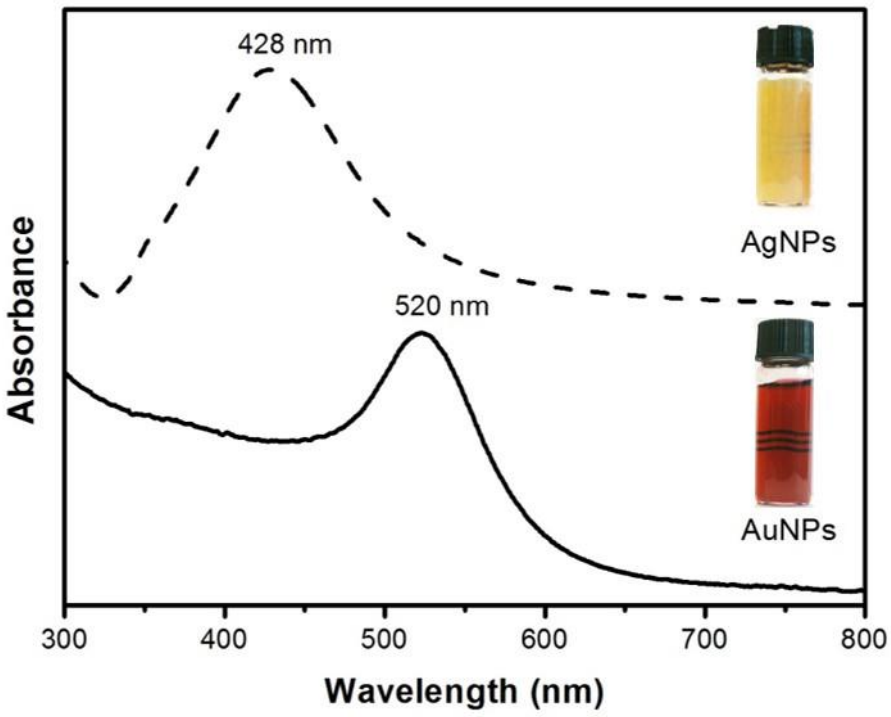

Figure 17. UV-VIS spectrum of Au and Ag NPs.

The intense peak at 520 nm for AuNPs can be attributed to the surface plasmon excitation of small spherical AuNPs. On the other hand, AgNPs presented a broad absorbance band with a maximum at 428 nm, indicating larger sized AgNPs with a wide size distribution.

The metallic NPs were also characterized by spectroscopy analysis such as Fourier Transform Infrared spectroscopy (FTIR) to study the molecular species attached at the surface of Au and Ag NPs (Figure 18).

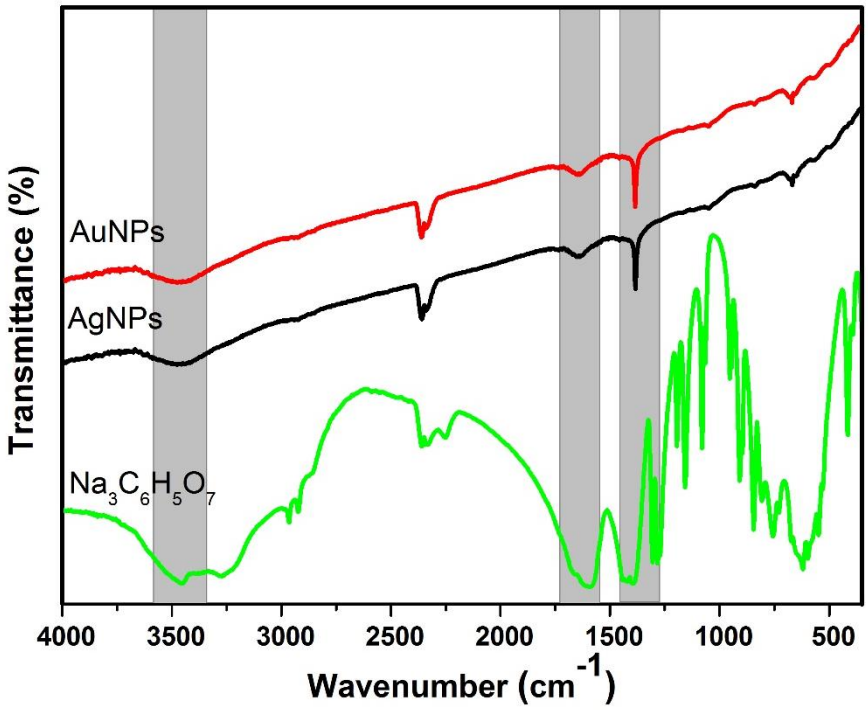

Figure 18. FTIR spectrum of synthesized Au and Ag NPs, indicating the adsorption of sodium citrate onto their structures through the presence of carboxylate symmetric and asymmetric stretching vibrations from citrate at ~1382 cm^{-1} and around 1500-1630 cm^{-1}, respectively.

The bands at ~1382 cm^{-1} and around 1500-1630 cm^{-1} are assigned as the carboxylate symmetric and asymmetric stretching vibrations from citrate, respectively [$\nu_{sym}(COO^-)$, $\nu_{asy}(COO^-)$]. The presence of two distinct symmetric and asymmetric stretching vibrations, $\nu_{sym}(COO^-)$ - $\nu_{asy}(COO^-)$, is indicative of the binding character of a carboxylate group with a metal ion, suggesting the coupling of citrate onto the surface of Au and Ag NPs. The band between 3550-3300 cm^{-1}corresponds to a characteristic stretching vibration of OH^- groups due to adsorbed water (H_2O) [2].

For the assessment of the stability of the colloids, Zeta Potential values were measured and were found to be -51.2 mV and -39.4 mV for Au and Ag NPs, respectively (Table 3). The negative Zeta potential measurements are due to the capping of citrate ions on the surface of metal structures. Both colloids (Au and Ag NPs) are stable accordingly with these results.

Table 3. Zeta Potential measurements.

	ζ (mV)	**pH**
AuNPs	-51.2	5.3
AgNPs	-39.4	7.4

The size and shape of the noble metal NPs were verified by Transmission Electronic Microscopy (TEM). Figure 21 presents the TEM micrographs of Au (a) and Ag NPs (b).

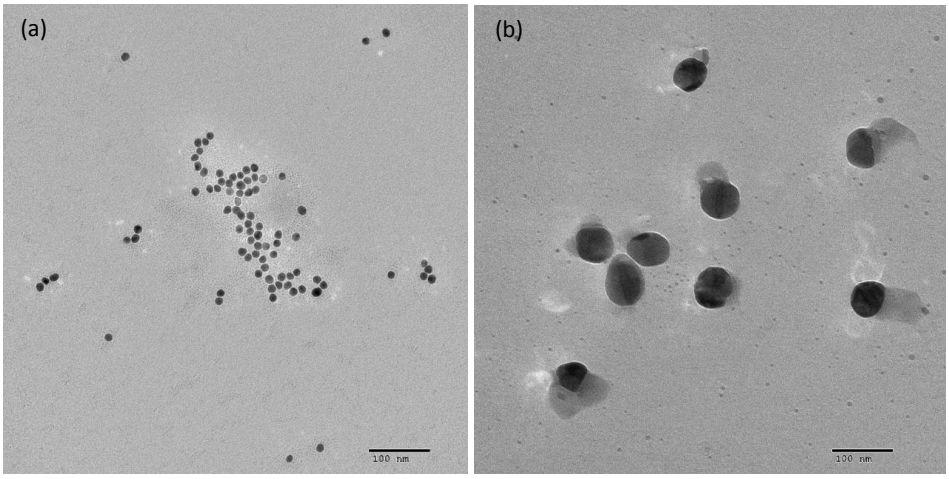

Figure 19. TEM micrographs of Au (a) and Ag NPs (b).

AuNPs synthesized by the citrate reduction method (Figure 19.a) exhibit indeed spherical and uniform-sized particles. The size distribution histogram obtained from the micrographs of the particles (Figure 20.a), fitted with a Gaussian curve, registered a mean diameter and standard deviation of 14.4 nm and 2.4 nm, respectively. Particles with diameters longer than 20 nm could have been resulting from some aggregation during preparation of the TEM holding grid.

AgNPs (Figure 19.b) also show nearly spherical morphology, but the size is bigger than AuNPs. The particle's size distribution histogram obtained from the micrographs presented a mean diameter of 54.2 nm and a standard deviation of 17.6 nm, respectively. As shown in the particle size distribution histograms (Figure 20.b), AgNPs present broad size distributions with particle sizes ranging from 20 to 100 nm.

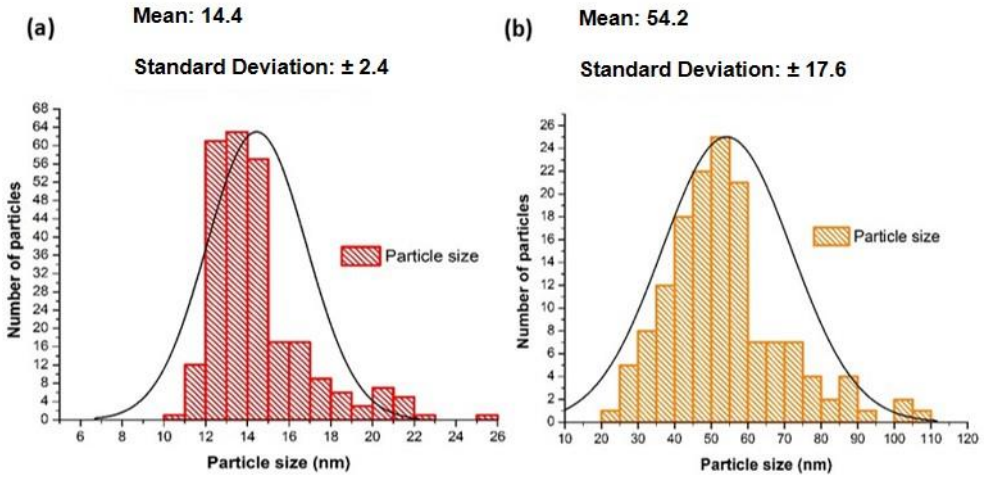

Figure 20. Particle size distributions of Au (a) and Ag NPs (b) using sodium citrate as the reducing agent.

The average number of Au and Ag atoms per nanoparticle (N) may be calculated from TEM analysis by knowing that $N=31d^3$ according to Liu *et al*., where d is the average core diameter (nm) of the nanoparticle obtained from the micrographs [3]. The molar concentration of AuNPs and AgNPs (C) was then calculated by dividing the total number of Au and Ag atoms added to their respective reaction solutions (N_{total}) over the average number of Au and Ag atoms per nanoparticle (N), following the equation (1)

$$C = \frac{N_{total}}{NVN_A} \qquad (1)$$

V is the volume of the reaction solution and N_A the Avogadro's constant (~6.02×10^{23}).It was estimated a concentration of 1.24×10^{-8} M for AuNPs and 2.02×10^{-10} M for AgNPs.

2.2. Seed-mediated growth

The need for synthesizing AuNPs with larger sizes, required the use of a slightly different synthetic route. The presented procedure consisted in the synthesis of AuNPs through the mediated-seed growth method, by using sodium citrate and ascorbic acid as reducing agents. In this procedure, smaller particles acted like seeds for later particle enlargement. The increase in the size of AuNPs can be witnessed by the change in the colour of the colloids which goes from cherry-red in the first step, through ruby-red in the second to a light pink in the last growth step (Figure 21).

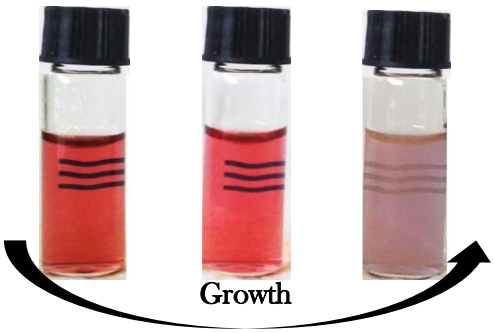

Figure 21. AuNPs obtained experimentally via seed growth method.

UV-VIS and microscopy analysis were performed to study the size and morphology of the synthesized AuNPs. Figure 22 shows the UV-VIS absorbance of AuNPs obtained at different growth steps.

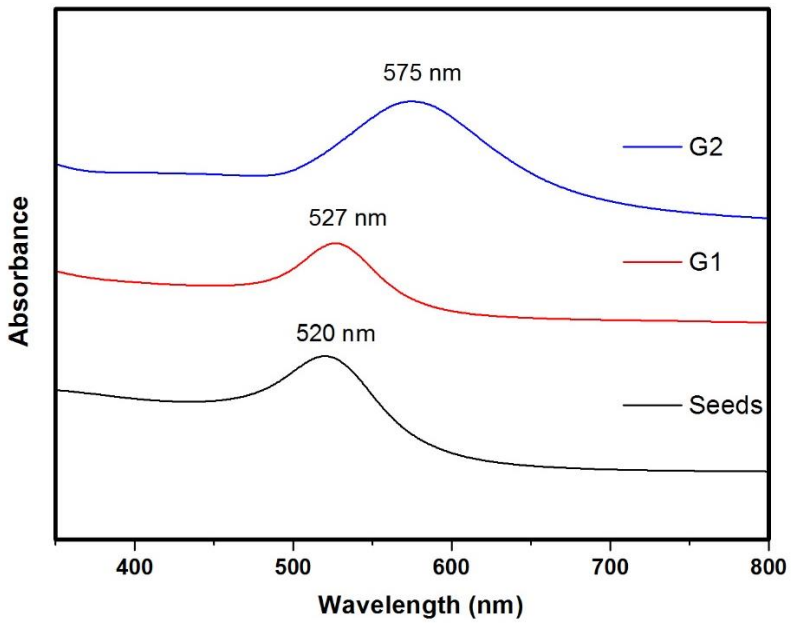

Figure 22. UV-VIS spectra of AuNPs at different growth steps (seeds, G1 and G2).

The sharp absorbance peaks for the Au seeds and for the first growth step, G1, located nearly at 520 nm and 527 nm, respectively, are caused by the presence of small and uniform-sized spherical NPs with narrow size distributions. In the second growth step, G2, absorbance shows a red shift of ~50 nm, indicating a considerable increase in the size of AuNPs.

Although the size and shape of NPs is generally determined by TEM, UV-VIS spectra can also be used to obtain preliminary estimates of the size and concentration of NPs in aqueous solutions [4].

The size and concentration of AuNPs can be calculated with reference to Haiss *et al* [5]. According to Haiss, when AuNPs have diameters smaller than 35 nm, the ratio of the absorbance at the SPR peak to the absorbance at 450 nm can be used to determine the particle size without knowing the concentration using the following equation:

$$d = exp\left(B_1 \frac{A_{spr}}{A_{450}} - B_2\right) \qquad (2)$$

where A_{spr}/A_{450} is the ratio of the absorbance at the surface plasmon resonance peak (A_{spr}) to the absorbance at 450 nm (A_{450}), $B_1 = 3.00$ and $B_2 = 2.20$ and d is the diameter.

For NPs with sizes ranging from 35 to 120 nm, Haiss presents a different equation:

$$d = \frac{ln\left(\frac{\lambda_{spr} - \lambda_0}{L_1}\right)}{L_2} \qquad (3)$$

where d is the diameter of a nanoparticle, and λ_{spr} is the plasmonic peak wave. $\lambda_0 = 512$, $L_1 = 6.53$ and $L_2 = 0.0216$ are fitting parameters determined from the theoretical values.
The concentration of AuNPs was also determined by using the diameters estimated in (2) and (3) and accordingly with the literature [4, 5]. Table 4, summarizes the results obtained from the UV-VIS spectra.

Table 4. Results obtained from UV-VIS following Haiss equations.

Growth step	Diameter (nm)	Concentration (NPs/ml)	Concentration (Mol/l)	SPR peak (nm)	A_{spr}	A_{450}
Seeds	14.3	1.5×10^{12}	2.3×10^{-4}	520	0.76601	0.47145
G1	38.5	6.2×10^{10}	1.8×10^{-4}	527	0.88753	0.44421
G2	104.9	4.0×10^{9}	2.4×10^{-4}	575	1.08437	0.46574

Figure 23 illustrates Transmission Electron Microscopy (TEM) and Scanning Transmission Electron Microscopy (STEM) micrographs of the as-prepared AuNPs together with the particle size distribution histograms generated from the micrographs.

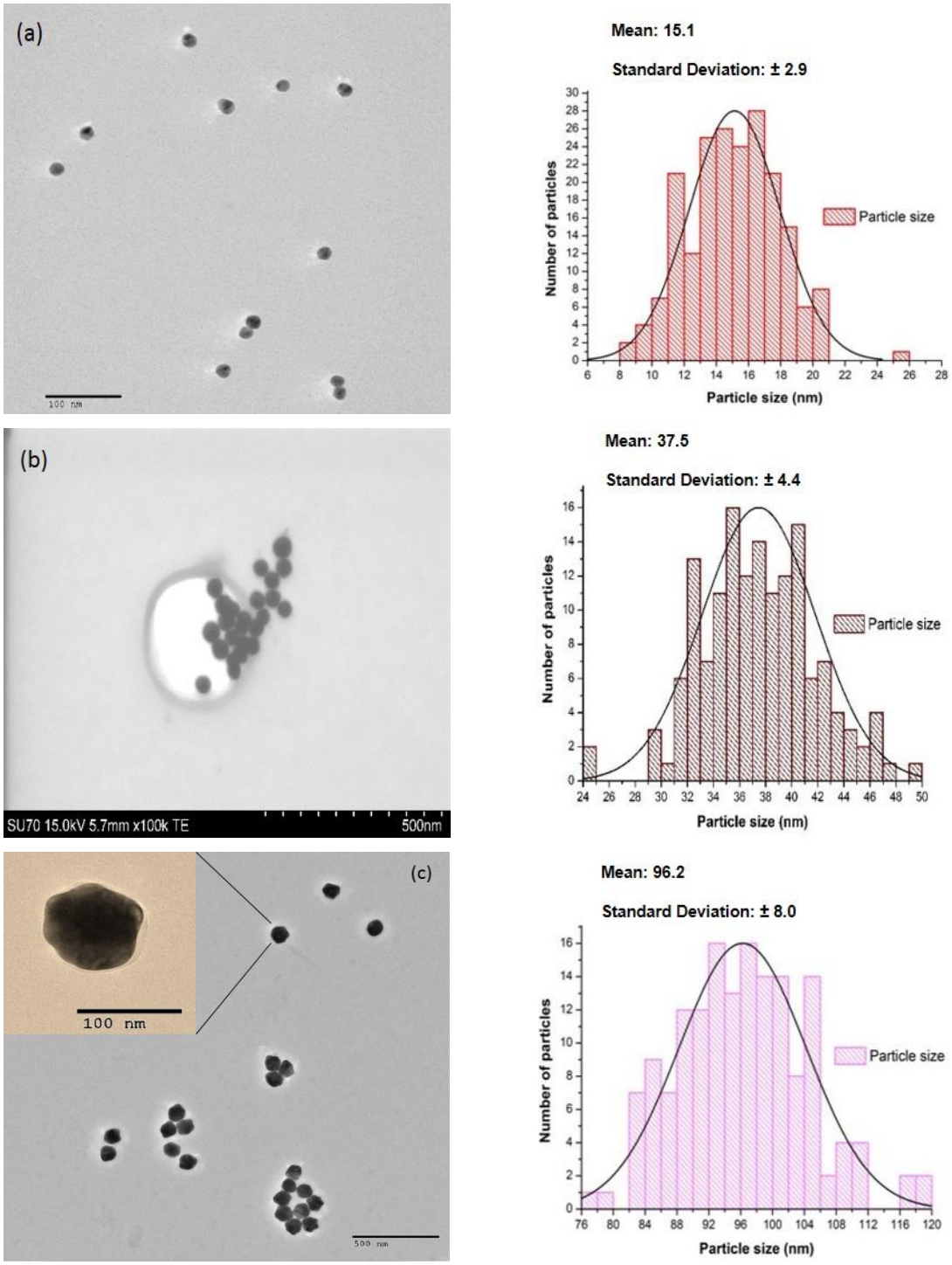

Figure 23. (a) TEM micrograph of Au seeds; (b) STEM micrograph of AuNPs of the first growth step, G1; (c) TEM micrograph of AuNPs of the second growth step. The insert is a higher magnification micrograph of AuNPs of the second growth step with a scale bar of 100 nm.

Au seeds present uniform sizes and narrow size distributions as confirmed by TEM micrographs and respective particle size distribution histogram (Figure 23.a). They exhibited spherical shapes with an average diameter of 15.1 nm (standard deviation of 2.9).

AuNPs of the first growth step continued to demonstrate good spherical shapes and narrow size distributions (particle sizes range mainly from 29 to 50 nm). (Figure 23.b) The size of the nanoparticle found in STEM was 37.5 nm (standard deviation of 4.4), which is in good agreement with the calculated value (38.5 nm) in reference to Haiss.

Finally, TEM confirmed that AuNPs of the second growth step are not quite spherical at this stage but instead present some facets and edges. These NPs have a particle mean size of 96.2 nm (standard deviation of 8.0), approximately 8 nm smaller than the theoretical value obtained with the Haiss calculations (Figure 23.c) There is also a broadening of the particle size distribution, which is congruent with the wide absorbance peak obtained from the UV-VIS analysis.

2.6. References

[1] Turkevich, J., Stevenson, P. C., and Hillier, J., "A study of the nucleation and growth processes in the synthesis of colloidal gold", *Discussions of the Faraday Society,* vol. 11, pp. 55-75, 1951.

[2] Park, J. W. and Shumaker-Parry, J. S., "Structural study of citrate layers on gold nanoparticles: role of intermolecular interactions in stabilizing nanoparticles", *Journal of the American Chemical Society,* vol. 136, pp. 1907-21, 2014.

[3] Liu, X., Atwater, M., Wang, J., and Huo, Q., "Extinction coefficient of gold nanoparticles with different sizes and different capping ligands", *Colloids and Surfaces B: Biointerfaces,* vol. 58, pp. 3-7, 2007.

[4] Maciulevičius, M., Vinčiūnas, A., Brikas, M., Butsen, A.*, et al.*, "Pulsed-laser generation of gold nanoparticles with on-line surface plasmon resonance detection", *Applied Physics A,* vol. 111, pp. 289-295, 2013.

[5] Haiss, W., Thanh, N. T. K., Aveyard, J., and Fernig, D. G., "Determination of Size and Concentration of Gold Nanoparticles from UV-Vis Spectra", *Analytical Chemistry,* vol. 79, pp. 4215-4221, 2007.

“I have not failed 700 times. I have not failed once. I have succeeded in proving that those 700 ways will not work. When I have eliminated the ways that will not work, I will find the way that will work.”

Thomas Edison

Chapter 3

Results and Discussion

3. Results and discussion

In a first approach it was performed a simple and direct label-free detection method by applying cardiac troponin I onto the surface of Au and Ag NPs. This step is of crucial importance because allows to investigate structural aspects of the full-length cardiac troponin I that are absent of any XRD data and less studied from a surface chemistry and spectroscopy perspective. Additionally, an exhaustive study of its spectrum allowed to understand inherent biodetection issues that will be of great value for future optimization of experimental conditions.

The SERS spectrum provides a fingerprint which represents the set of bonds present in the protein. The vibrational frequencies are characteristic of the chemical bonds and groups of bonds between different amino acids (the building blocks of peptides and proteins). These vibrational frequencies are sensitive to details of the structure and local environment of the protein such as symmetry, crystal phase, interaction and orientation, etc [1]. For instance, groups in the protein such as the carboxyl group (COOH) or amino groups (NH_2) interact with the metal surfaces, giving strong enhancements of these bands. Other spectral features of proteins typically include bands from aromatic side chain vibrations of amino acids like tyrosine, tryptophan and phenylalanine and also from disulphide bridges (S-S) between pairs of cysteine residues [2].

Disulphide bonds in proteins are covalent bonds formed between thiol groups (-SH) present in cysteine residues (Figure 24). S-S bonds are essential for the functional properties of proteins and are key elements in the stabilization of tertiary structures [3, 4].

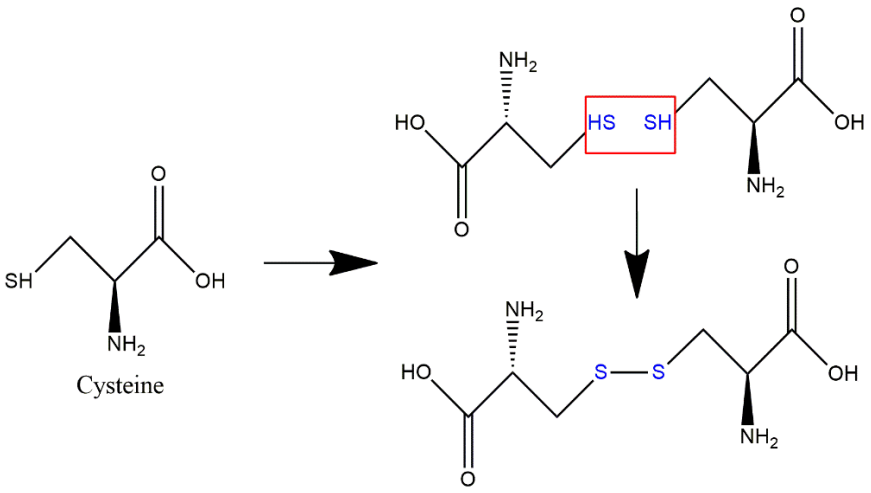

Figure 24. Thiol groups of free pairs of cysteine residues can form disulphide bonds (S-S), playing a major role in protein tertiary and quaternary structures.

Since certain amino acids such as cysteine contain thiol groups within its structures, these compounds could be easily chemisorbed onto the surface of metallic NPs due to high affinity with metal, thus providing strong enhanced bands in the spectra. Hence, it was expected that the presence of cysteine residues would be favourably observed in the spectra of both metallic NPs.

SERS analysis started with the addition of cardiac troponin I onto the surface of the colloids (Au and Ag) synthesized via citrate reduction method. The spectra of the substrates were also recorded in SERS prior to the detection of the protein on each assay to better perceive spectral differences that are only derived from the protein.

Figure 25 displays the SERS spectra of cardiac troponin I onto the surface of 15 nm AuNPs.

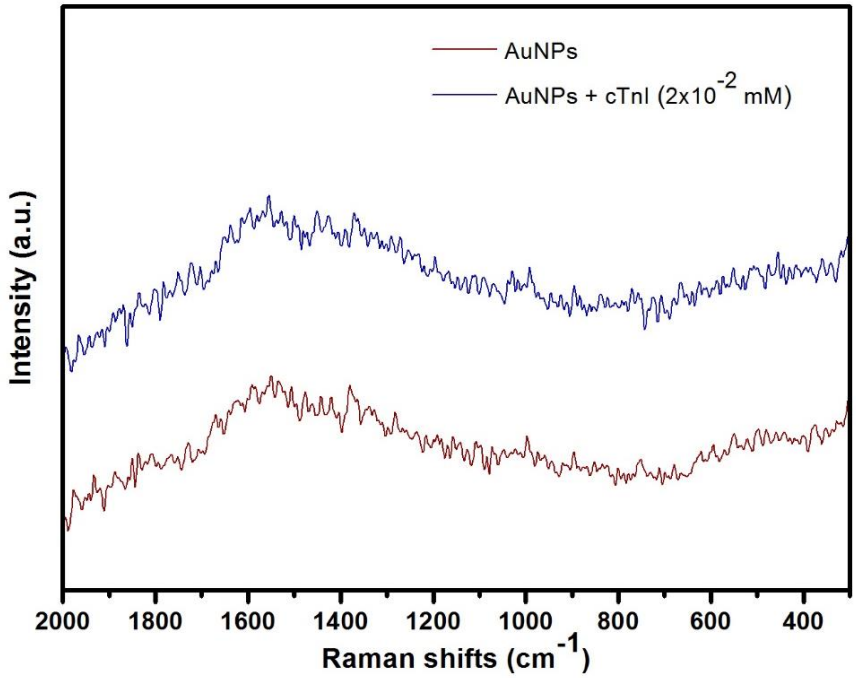

Figure 25. Spectra of cardiac troponin I onto the surface of AuNPs (blue colour). The spectra of the colloid (red colour) was also performed as a reference.

After observation of the spectra, it is possible to confirm that there is no single peak formation and therefore no evidence of detection of cardiac troponin I. The spectra of cardiac troponin I exhibits plenty of noise and it is substantially equivalent to the spectra of the substrate alone which indicates the inexistence of some sort of detectable signal from the protein.

On the other hand, when cardiac troponin I was applied directly to the surface of 50 nm AgNPs synthesized similarly by the same method the response was different. In this case, it is possible to observe intense bands nearly at 400, 630, 720, and 1009 cm^{-1} (Figure 26).

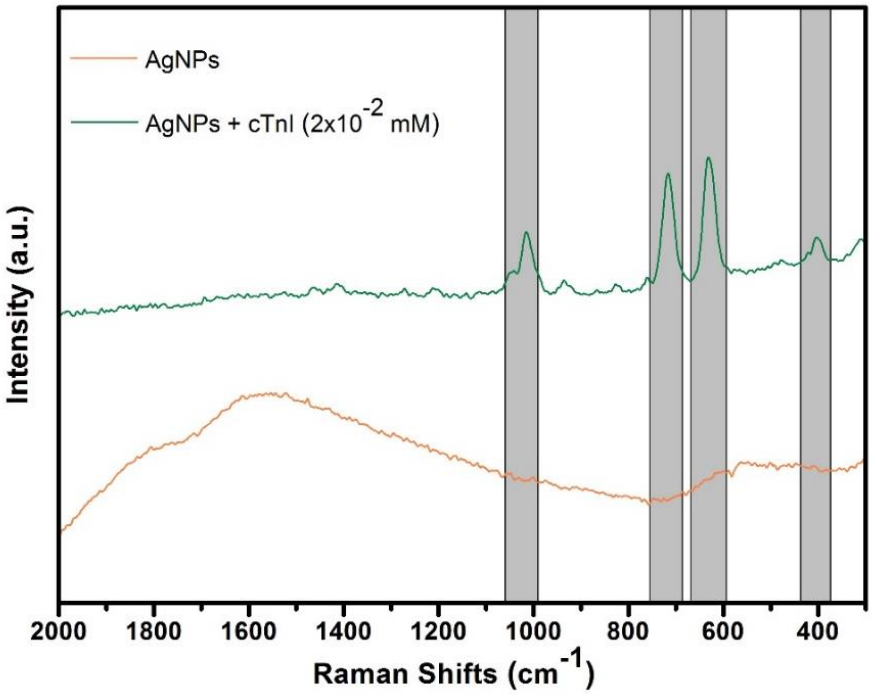

Figure 26. Spectra of cardiac troponin I onto the surface of AgNPs (green colour). The spectra of silver colloids was considered as a reference.

These results are not conclusive so far in part because cardiac troponin I was acquired within a considerable amount of a preservative stabiliser known as 2-mercaptoethanol. 2-Mercaptoethanol is used to break disulphide bonds (S-S) in proteins, leading to the disruption of both quaternary and tertiary structures [5]. 2-Mercaptoethanol is often included in several enzyme assays as a standard buffer solution to maintain protein activity by inhibiting oxidation (loss of H^+) of free sulfhydryl residues [6]. Figure 27 illustrates the mechanism of cleavage of disulphide bonds of cysteine residues by using 2-mercaptoethanol.

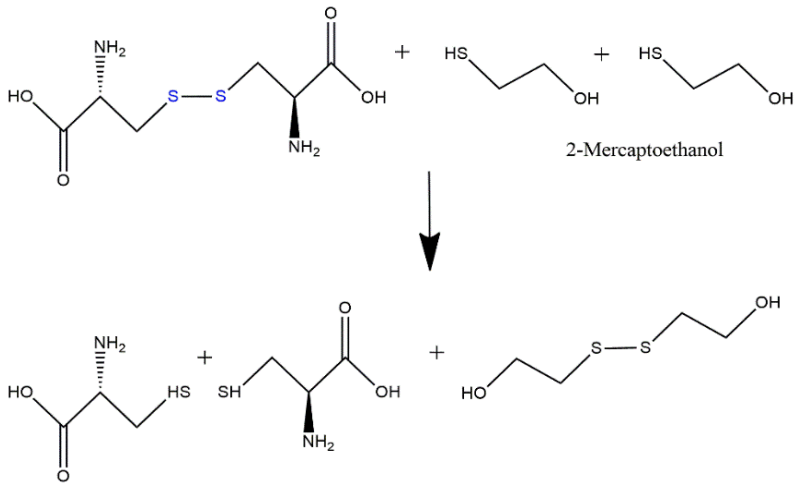

Figure 27. 2-mercaptoethanol breaking disulphide bonds (S-S) and preventing oxidation (loss of H^+) of sulfhydryl groups (-SH).

We know that 2-mercaptoethanol is embedding cardiac troponin I in a concentration of 15 mM, so it is possible that the resulting spectrum could be derived from the adsorption of 2-mercaptoethanol onto the surface of AgNPs instead of cardiac troponin I. To confirm the suspicion of the adsorption of 2-mercaptoethanol onto the surface of AgNPs, the spectra of 2-mercaptoethanol was also performed as shown in Figure 28.

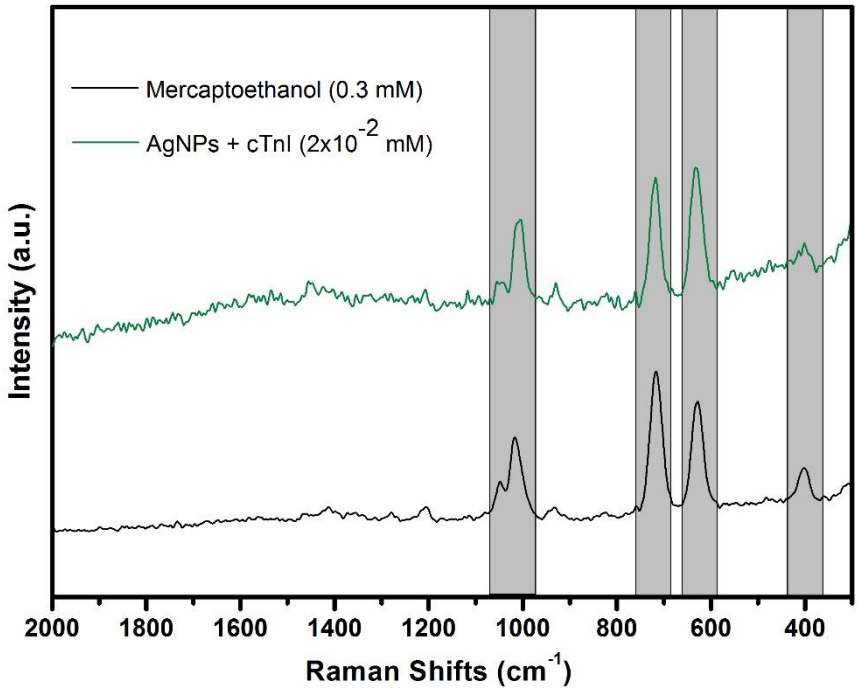

Figure 28. Spectra of cardiac troponin I with AgNPs and 2-mercaptoethanol.

There is a perfect match between the spectra of 2-mercaptoethanol and the spectra of the presumably adsorbed cardiac troponin-I onto the surface of Ag NPs. Furthermore, these results are consistent with previous reports in the literature related with the chemisorption of 2-mercaptoethanol on metal structures [7]. The strongest Raman bands for the adsorbed 2-mercaptoethanol molecules are at 639 and 720 cm^{-1} assigned to the C-S stretching, and about 1009 cm^{-1} due to out-of-phase C-C-O stretching. The presence of a weak band at 400 cm^{-1} is assigned to the C-C-O bending vibration.

Despite the presence of such an obstacle, it was unintentionally found in this work that 2-mercaptoethanol had more affinity to AgNPs rather than AuNPs. This could have been influenced by differences in metal-S bonding or to the character and geometry of the sulphur-substrate bonding or even due to differences in size of the NPs [7, 8]. AgNPs were considerably larger than AuNPs (with an average diameter of 54.2 nm versus 14.4 nm for AuNPs). This result may be consistent with some reports indicating that larger sized NPs are shown to preserve disulphide bonds and for that reason are considered as the most appropriate substrates for ensuring the integrity of disulphide linkages [8].

In order to continue with SERS measurements it was necessary to filtrate the protein, thus eliminating possible interferences resulting from the adsorption of 2-mercaptoethanol on the surface of both metallic NPs. After filtration, the “pure” cardiac troponin I (initial concentration of 5×10^{-3} mM) was added again to the surface of both metallic NPs for further analysis. Figure 29 shows the resulting spectra of pure cardiac troponin I in different substrates.

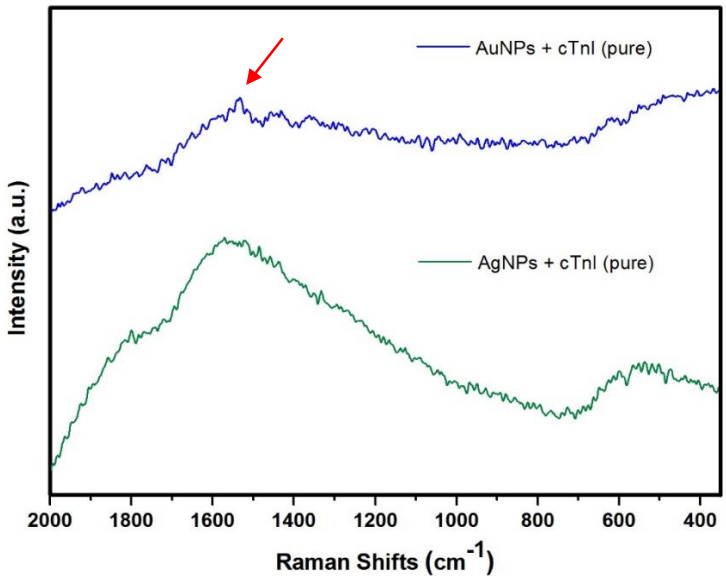

Figure 29. Spectra of the filtered cardiac troponin I on Au and Ag NPs. Peak evidence near 1533 cm^{-1} when using AuNPs.

The spectra presented in Figure 29 do not show any evidence of 2-mercaptoethanol onto the surface of AgNPs, which indicates that the separation technique was apparently successful. There are no significant differences between the spectra of cardiac troponin I and the spectra of silver colloids. On the other hand, it is possible to identify a small band nearly 1533 cm^{-1} in the case of using AuNPs as substrates. This result aroused curiosity around the existence of such band and clearly showed that AuNPs may be a good candidate to be used as SERS substrate for the detection of this protein. However, it is important to note that the spectra of cardiac troponin I using AuNPs with 15 nm also showed bad resolution and poorly defined peaks, even with increased time scans. So, in order to improve the Raman signal of the protein and to get stronger band enhancements, the solution aimed for the increase of the size of the nanoparticle. It is known that when the nanoparticle diameter increases, the plasmon resonance shifts to higher wavelengths (getting closer to the laser's irradiation source) leading to significant larger light-interaction cross-sections which greatly increases the scattering efficiency.

Obviously, the next tests were performed using AuNPs with sizes around 35 and 96 nm synthesized via seeding growth method. Figures 30 and 31 present the spectra of cardiac troponin I with different sized AuNPs as SERS platforms.

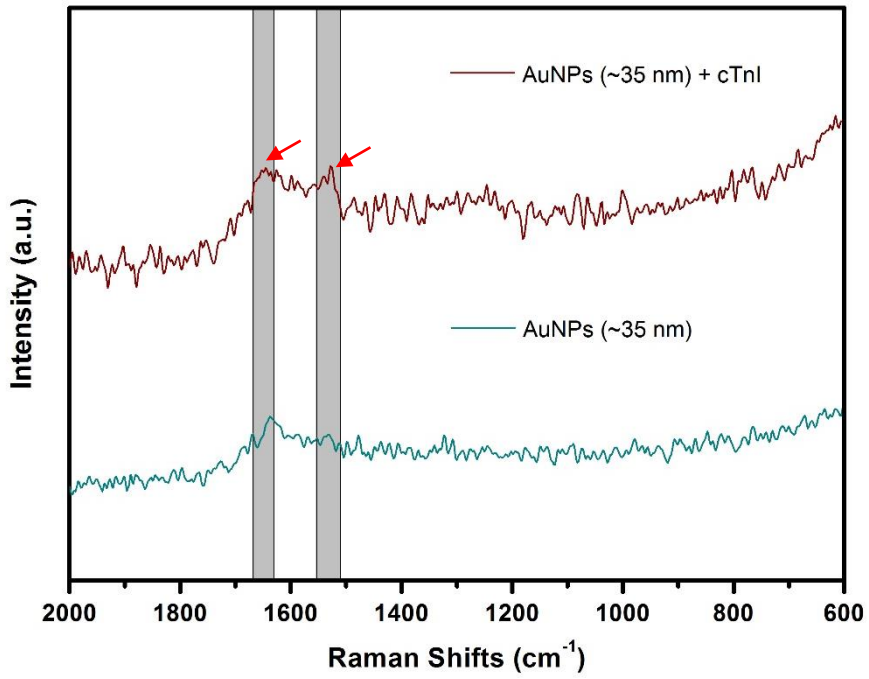

Figure 30. Spectra of cardiac troponin I on the surface of AuNPs with sizes around 35 nm.

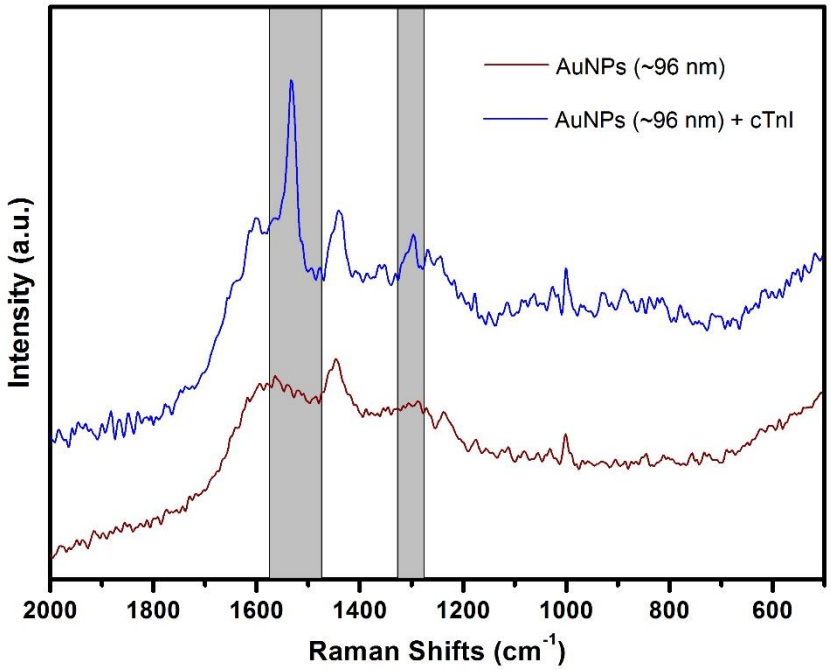

Figure 31. Spectra of cardiac troponin I on the surface of AuNPs with sizes around 96 nm.

The spectra of the figures 30 and 31 show characteristic bands of peptides and including amide I, II and III bands [9]. The amide bands arise due to bond vibrations in the peptide units [10]. For instance, when two amino acids such as alanine and glycine are combined together, a molecule of water is eliminated to produce a dipeptide (Figure 32).

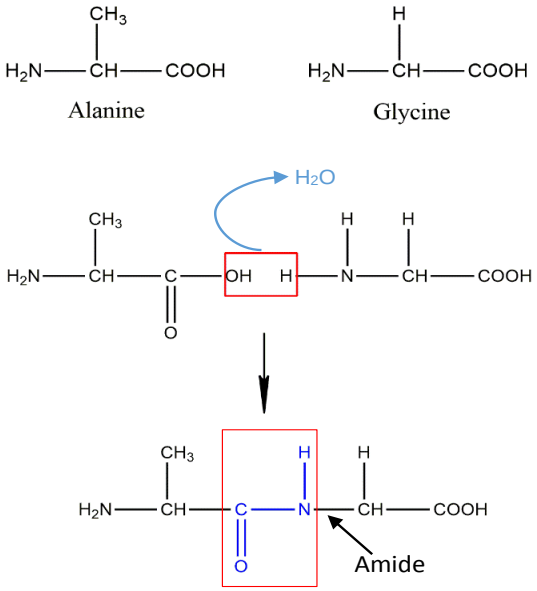

Figure 32. Formation of an amide link between two amino acids by elimination of one molecule of water.

The linkage highlighted in blue in the structure of the dipeptide is known as a peptide or amide link whose vibrational frequencies, in this case, are being detected by SERS.

The amide I band is typically found in the spectra region of 1700-1600 cm^{-1}. The amide I band consists of C=O stretching vibrations with some contribution from N-H bending [11, 12]. The amide II is usually found in the 1520 and 1540 cm^{-1} region and results from in-plane N-H bending and from the C-N stretching vibration [13, 14]. Finally, the amide III band is found in the region of 1240-1310 cm^{-1} and results from stretching of C-N and N-H bending vibrations [14]

In the SERS of cardiac troponin I as shown in figure 30 the amide bands appear at nearly 1642 cm^{-1} (amide I) and 1533 cm^{-1} (amide II). When the size of AuNPs increases from 35 to 96 nm, the most noticed bands are the amide II at 1533 cm^{-1} and the amide III at 1298 cm^{-1}, as shown in figure 31. It is worth noting that the amide II band is consistent with previous results and may be found in every spectra so far. The intensity of this band is strongly enhanced when the size of AuNPs is further increased.

The amide II band was still identified without causing aggregation of particles with magnesium chloride ($Mgcl_2$) as shown in figure 33. $Mgcl_2$ was used throughout the work to cause aggregation of particles and to deliberately induce the formation of Hot-Spots in order to get greater signals by strong electromagnetic enhancements near metal junctions.

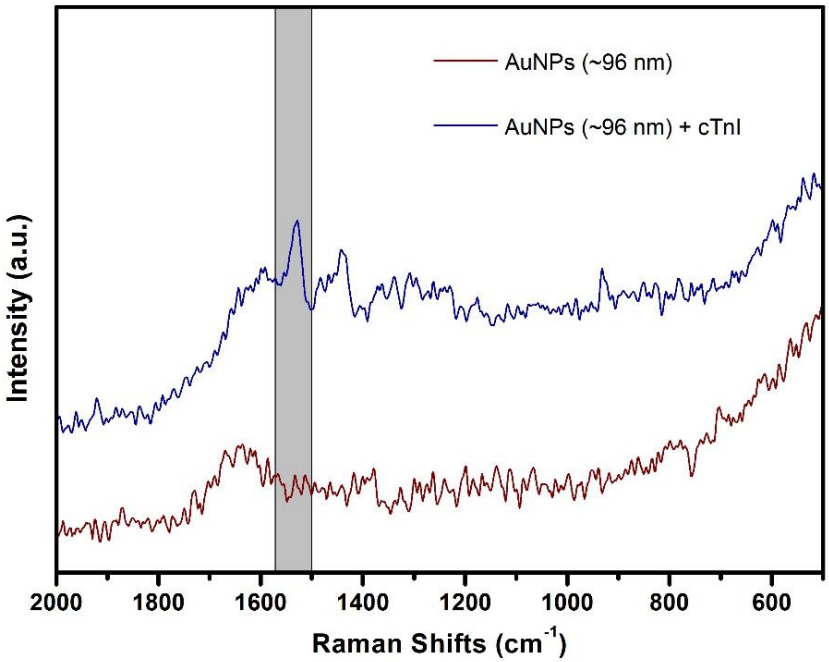

Figure 33. Spectra of cardiac troponin I without the addition of magnesium chloride.

The detection limit of cardiac troponin I was also studied with different sample concentrations (initial concentrations of 1×10^{-2}, 1×10^{-3}, 1×10^{-4} mM) as shown in figure 34.

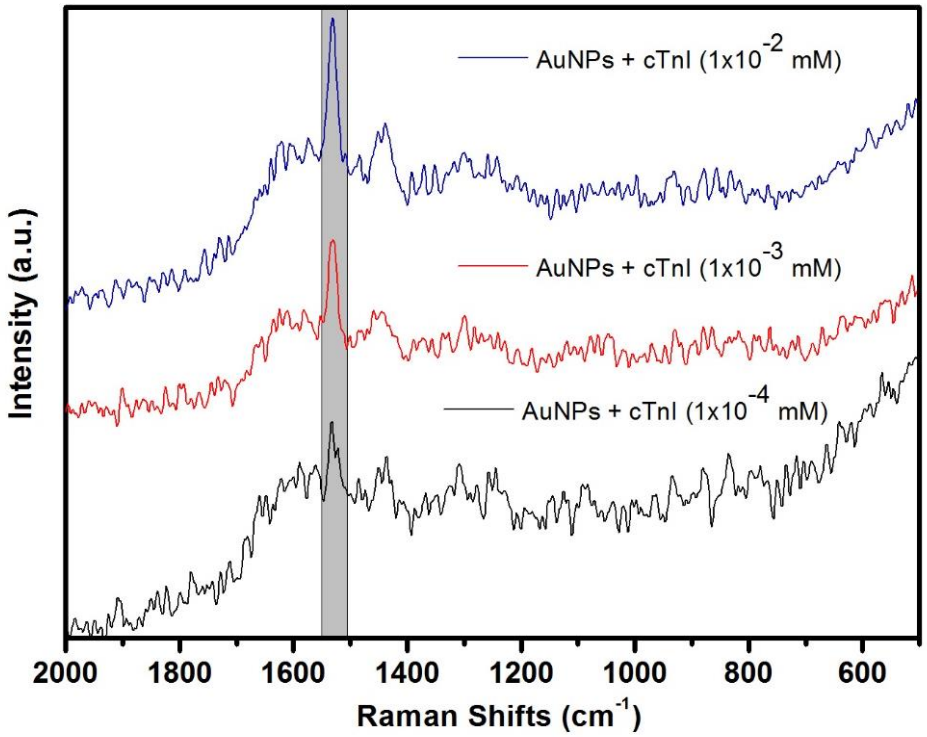

Figure 34. Spectra of cardiac troponin I with different initial concentrations (1×10^{-2}, 1×10^{-3}, 1×10^{-4} mM).

This result suggests that the concentration of cardiac troponin I is indeed decreasing with more sample dilutions, which is in accordance with the decrease in the intensity of the spectra. If there was not any protein at all the spectra would have remained unaltered and with the same intensity because the only variable of the system is the concentration of the protein. Unfortunately, it was not possible to detect bands from aromatic side chain vibrations of amino acids such as phenylalanine, tryptophan or from SH/S^- linkages between cysteine residues and the metal surface.

Considering the hypothesis of the total removal of 2-mercaptoethanol during filtration, it is possible that, at alkaline pH, the protein rapidly undergoes reoxidation to form the original disulphide bonds, thus preventing the adsorption of these amino acids to the metal surface.

On the other hand, if there is still some amount of 2-mercaptoethanol it is also probable that 2-mercaptoethanol has formed some adducts with free cysteine residues, causing instability and interferences with protein-metal interactions. These factors could have contributed to inhibit some kind of interaction between cysteine residues and the metal surfaces. The non-identification of other amino acids in the spectrum could also be attributed to the distance of a certain moiety from the metal surface. If the polarizable part of some functional groups are distanced or not oriented towards the metal surface, it will be more difficult to be observed in the Raman spectra. That is why it is of great interest the functionalization of metal surfaces with biomolecules because they are capable to bind to specific targets, providing a specific Raman signal due to the interaction of the biomolecule with the target molecule.

Since unmodified AuNPs were prepared through the classical citrate-reduction method and are loosely capped by negatively charged citrate ions they show high affinity to positively charged molecules and much less affinity to negatively charged ones. As a result, pH changes also may dictate interactions with some amino acids. The pH of ~ 35 and 96 nm Au colloids was nearly 3.0. The low pH of AuNPs is due to the use of citric and ascorbic acids during the seeding-mediated growth method. When adding cardiac troponin I the pH increases to nearly 4. At this pH, the amino group in cysteine is positively charged and could interact with the negative charge on the surface of gold. However, in this work neither SH nor NH_3^+ of cysteine were bound with metal ions.

Nevertheless, it was possible to identify amides with a simple intrinsic SERS configuration. The detection of amides could be attributed to the overall contribution from each and every amide summed, thus providing detectable signals with strong enhancements.

3.1. References

[1] Shanmukh, S., Jones, L., Driskell, J., and Zhao, Y., "Rapid and sensitive detection of respiratory virus molecular signatures using a silver nanorod array SERS substrate ", *Nano Letters,* vol. 6, pp. 2630-2636, 2006.

[2] Siddhanta, S. and Narayana, C., "Surface Enhanced Raman Spectroscopy of Proteins: Implications for Drug Designing", *Nanomaterials and Nanotechnology,* vol. 2, pp. 1-13, 2012.

[3] Thangudu, R. R., Manoharan, M., Srinivasan, N., Cadet, F*., et al.*, "Analysis on conservation of disulphide bonds and their structural features in homologous protein domain families", *BMC Structural Biology,* vol. 8, p. 55, 2008.

[4] Hogg, P. J., "Disulfide bonds as switches for protein function", *Trends in Biochemical Sciences,* vol. 28, pp. 210-214, 2003.
[5] Lundblad, R. L., *Techniques in protein modification,* 1995.
[6] Deng, K., Huang, Y., and Hua, Y., "Isolation of glycinin (11S) from lipid-reduced soybean flour: effect of processing conditions on yields and purity", *Molecules,* vol. 17, pp. 2968-79, 2012.
[7] Kudelski, A., "Chemisorption of 2-Mercaptoethanol on Silver, Copper,and Gold: Direct Raman Evidence of Acid-Induced Changes in Adsorption/Desorption Equilibria", *Langmuir,* vol. 19, pp. 3805-3813, 2003.
[8] López-Tobar, E., Hernández, B., Ghomi, M., and Sanchez-Cortes, S., "Stability of the Disulfide Bond in Cystine Adsorbed on Silver and Gold Nanoparticles As Evidenced by SERS Data", *The Journal of Physical Chemistry C,* vol. 117, pp. 1531-1537, 2013.
[9] Vidal Bde, C. and Mello, M. L., "Collagen type I amide I band infrared spectroscopy", *Micron,* vol. 42, pp. 283-9, 2011.
[10] Montalbetti, C. A. G. N. and Falque, V., "Amide bond formation and peptide coupling", *Tetrahedron,* vol. 61, pp. 10827-10852, 2005.
[11] Yucel, T., Cebe, P., and Kaplan, D. L., "Structural Origins of Silk Piezoelectricity," *Advanced Functional Materials,* vol. 21, pp. 779-785, 2011.
[12] Moyo, M., "Horseradish Peroxidase Biosensor to Detect Zinc Ions in Aqueous Solutions", *Open Journal of Applied Biosensor,* vol. 03, pp. 1-7, 2014.
[13] Arsov, Z. and Quaroni, L., "Detection of lipid phase coexistence and lipid interactions in sphingomyelin/cholesterol membranes by ATR-FTIR spectroscopy," *Biochimica et Biophysica Acta,* vol. 1778, pp. 880-9, 2008.
[14] Litvinov, R. I., Faizullin, D. A., Zuev, Y. F., and Weisel, J. W., "The alpha-helix to beta-sheet transition in stretched and compressed hydrated fibrin clots", *Biophysical Journal,* vol. 103, pp. 1020-7, 2012.

Chapter 4

Conclusions and future work

4. Conclusions and future work

In this thesis it was given the first step towards the development of a novel SERS-based aptasensor. SERS is a powerful microanalytical tool that provided information about the set of bonds between the different amino acids that compose cardiac troponin I. SERS spectra showed evidence of a possible detection of cardiac troponin I with a simple intrinsic SERS configuration by identifying characteristic bands of peptides and proteins such as amide bands. The presence of cardiac troponin I (even in such trace amounts) was indeed confirmed with the decrease of the detectable signal with more sample dilutions.

AuNPs seem to be good candidates as SERS substrates for the detection of cardiac troponin I rather than AgNPs. As stated in this thesis, larger NPs are most suitable for biodetection purposes due to larger scattering cross-sections. The preferred adsorption of 2-mercaptoethanol on the surface of AgNPs indicated that larger sizes may eventually foster metal-S interactions more easily.

The presented work not only showed good insights for application of SERS in the area of clinical diagnosis, but also allowed to meet and deal with biodetection conundrums. In fact, much was learnt from circumstantial mistakes. For instance, the amount of cardiac troponin I (10 µg) was too low to make initial experiments, restraining any attempts of making other deeper spectroscopic studies. Next tests must be made with superior protein quantities. This will grant more access towards more environmental and structural data about cardiac troponin I, starting for example with the acquisition of the full spectrum of the native protein.

The next cardiac troponin I to be supplied must be on its native form and without any kind of preservative stabilizers. Studies must be made by using cardiac troponin I as if it was directly removed from the blood. Research focus must be closer to these clinical details. Even if there are indicators that confirm the detection of cardiac troponin I with these SERS substrates, more work needs to be done to sustain previous statements, but this time by fusing an aptamer as a crosslink to the protein. Aptamers will play a major role in the specific detection of cardiac troponin I. They will make the technology absolutely unique and differentiated from competitors.

The strategy of functionalization will be based on the introduction of a SH group at one end of the aptamer, leaving the other end directed to the outer-surface for specific interaction with cardiac troponin I. The process of functionalization is schematized in the following figure (Figure 35).

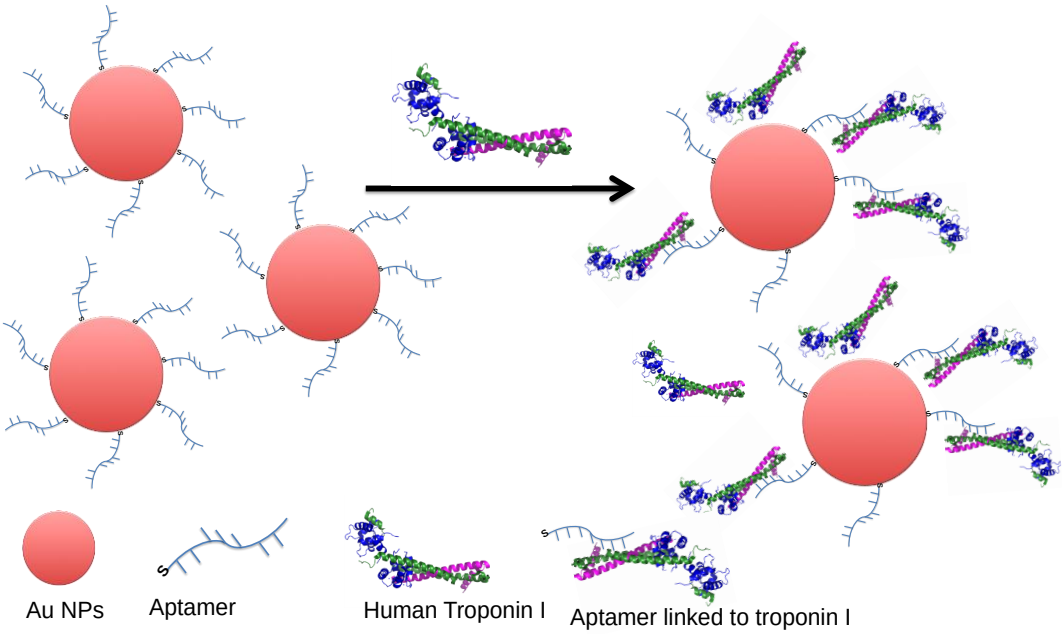

Figure 35. Preparation steps of the SERS-based aptasensor for the detection of cardiac troponin I. A thiol-modified aptamer is attached to the surface of the gold nanoparticles through gold-thiol bonds. In the presence of troponin I, the aptamer changes its conformation, binding with high affinity to cardiac troponin I.

Once completed the stage of functionalization, technology validation will be achieved by showing that circulating levels of troponin are detected within the required specificity and sensitivity ranges. This step should be performed by attaching thiolated-aptamers on metallic NPs with different shapes, sizes and compositions. If sensitivity needs to be lowered, there is a need for the pursuit of the ideal substrate. It is possible that the interaction between aptamers and metallic substrates may only function with a certain type of size or shape of NPs. There is an infinite “room” of possibilities to explore “at the bottom”!

It is envisaged that the presented SERS-based aptasensor will have potential for the improvement of both sensitivity and specificity in future biosensing applications, making it widely conveyable to other relevant health challenges such as pathogen detection, cancer diagnosis, auto-immunity disorders…

The potential of SERS for multiplexing will also be under study since it enables the measurement of multiple analytes in one single assay, another unique and truly innovative advantage in comparison with competitors. This feature not only tremendously reduces the costs with several biomarker testing orders, but also saves time for more straightforward clinical approaches.

The investment in a portable solution with multiplexing capability and an easy-to-use interface, opens the possibility of adopting a domiciliary device, with a vast array of potential future applications. For example, a multidisciplinary team of health professionals, equipped with a portable device, could provide a multitude of home services (e.g. diagnostics, screening tests, therapeutic control), or it could be rented to pharmacies or for private use, as appropriate.

Chapter 5

Experimental

5. Experimental

5.1. Reagents

Hydrogen tetrachloroaurate (III) trihydrate, ≥ 99.9% ($HAuCl_4.3H_2O$), sodium citrate tribasic dehydrate, ≥ 99.0% ($Na_3C_6H_5O_7.2H_2O$) and silver nitrate, ≥ 99.8% ($AgNO_3$) were purchased from Sigma-Aldrich, citric acid 1-hydrate, 99.5% ($C_6H_8O_7.H_2O$) was purchased from Panreac and L(+)-ascorbic acid, 99.7% ($C_6H_8O_6$) was obtained from Riedel-de-Haën. TRIS (Hydroxymethyl)-aminomethane, 99.8-100.1% ($NH_2C(CH_2OH)_3$) obtained from Pharmacia Biotech, sodium chloride, 99.5% (Nacl) provided from Panreac Química, calcium chloride dehydrate, 99.5% ($Cacl_2.2H_2O$) and magnesium chloride hexahydrate, 99.8% ($Mgcl_2$) purchased from Merck and cardiac troponin I, ≥98% supplied from AbD Serotec. Milli-Q water and distilled water were used throughout the work.

5.2. Instrumentation

5.2.1 UV-VIS

UV-VIS spectrometry measures the degree at which light is absorbed by a medium at different wavelengths in the ultraviolet, visible and near infrared spectra [1]. This technique is used because Au and Ag NPs have strong plasmon resonance absorptions which are dependent on the size and shape of the particles [2]. Information on the average particle size can be obtained from the absorption maximum of the measured UV–VIS spectrum of the colloidal solution. The visible spectra of the colloids was recorded on a Jasco V-560 UV/VIS spectrophotometer using quartz cells.

5.2.2 Zeta Potential

Zeta potential analysis is a technique used to determine the surface charge of NPs in solution [3]. Almost all materials will spontaneously acquire a surface electrical charge when brought into contact with a liquid [4]. This charge may arise from some mechanisms such as ionization of surface groups, adsorption of charged species on the surface of the nanoparticle, among others. Since NPs possess a surface charge on their surface, they will attract a thin layer of ions of opposite charge, creating an electric double layer. The electric

potential at the boundary of the double layer is known as Zeta Potential of the particle with values typically ranging from +100 mV to -100 mV (Figure 36) [4, 5].

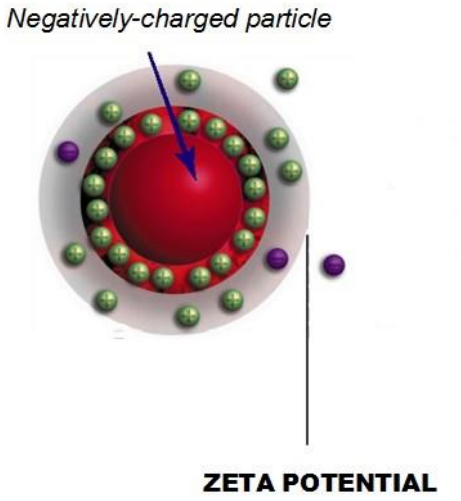

Figure 36. Illustration of Zeta Potential. Adapted from [5]

If all the particles in suspension have large positive or negative zeta potential then they will tend to repel each other and there will be no tendency for particles to come together. Therefore, the magnitude of the zeta potential is indicative of the stability of the colloidal system [6]. NPs with zeta potentials more positive than +25 mV or more negative than -25 mV are typically stable [7]. Colloids with lower values of zeta potential will eventually aggregate due to Van der Waals inter-particle attractions. Zeta Potential measurements were carried out on a ZetaSizer nano ZS Model Zen 3500 from Malvern Instruments using appropriate cells.

5.2.3 Fourier Transform Infrared Spectroscopy (FTIR)

FTIR is a technique based on the vibrations of the atoms in a molecule [8]. The infrared spectra is obtained by measuring the fraction of infrared radiation that is absorbed by the sample at a particular energy. The energy at which a peak appears in the spectrum corresponds to the frequency of a vibration of a part of a sample molecule.

FTIR spectra were recorded using a FT Mattson 7000 Spectrometer with resolution of 4 cm^{-1} after 256 scans. A few drops of colloid solutions were added to 200 mg of potassium bromide (KBr) and left to dry in an oven at 75ºC. The resulting solid residue was used to prepare pellets for FTIR analysis.

5.2.4 (Scanning) Transmission Electron Microscopy (TEM/STEM)

TEM/STEM can yield information such as particle size, size distribution and morphology of the NPs. The size of the NPs was directly observed and measured using a Hitachi SU-70 at an accelerating voltage of 15 kV (STEM) and a Hitachi H-9000 microscope operated at an accelerating voltage of 300 kV (TEM). STEM and TEM samples were prepared by placing a drop of the diluted colloids at room temperature on carbon-coated copper grids. Size distribution of the NPs was determined on the basis of the obtained micrographs with the use of the Image J program. The calculated sizes are expressed as the diameter of a sphere that has the same projected area as the projected image of the particle.

5.2.5 Surface-enhanced Raman Scattering (SERS)

Raman spectra were recorded using a Bruker RFS100/S FT- Raman spectrometer (Nd:YAG laser, 1064 nm excitation), at a power of 350 mV, with 500/1000 scans at a resolution of 2 cm^{-1}.

5.2.6 Amicon Ultra Centrifugal filters

Amicon Ultra 0.5 ml centrifugal filters, purchased from Sigma Aldrich, with a Molecular Weight Cut-Off (MWCO) of 3 kDa were used to remove 2-mercaptoethanol from cardiac troponin I.

5.3. Prior requirements for metallic nanoparticle synthesis

Firstly, all glassware was thoroughly washed prior to use with aquaregia solution (HCl: HNO_3 = 3:1) and rinsed with deionized water. The synthesis of metallic NPs was always carried out inside a well-ventilated Hotte.

5.4. Synthesis of Au and Ag NPs

AuNPs were synthesized by the reduction of hydrogen tetrachloroaurate (III) trihydrate ($HAuCl_4.3H_2O$) with sodium citrate dehydrate solution ($Na_3C_6H_5O_7.2H_2O$).

A 50 ml gold solution (1 mM) was prepared in a 2-neck round-bottom flask with the center neck attached to a reflux condenser. The flask was set in a hot plate with a magnetic stirrer to provide vigorous stirring and a thermometer was inserted to accurately measure the temperature of the solution. (Figure 37).

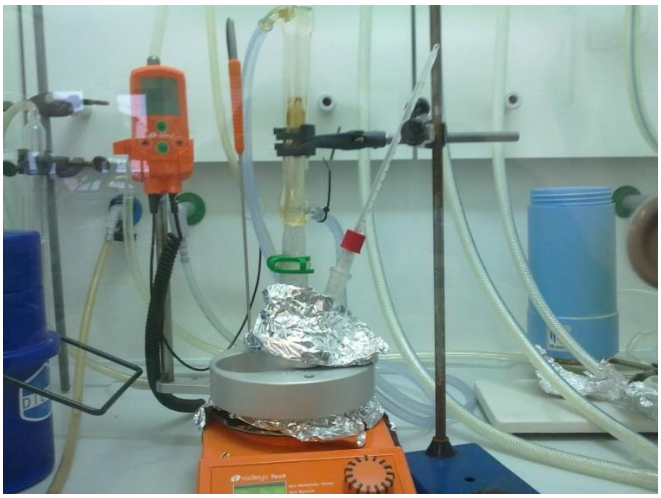

Figure 37. Metallic nanoparticle synthesis experimental setup.

A reflux condenser is used to cool down vapors arising from the solvent as they flow through the tube, leading to the condensation of the solvent. Since the condensed solvent falls back into the reaction vessel, any significant loss of volume of the solvent was prevented during the heating process.

When the solution almost reached its boiling point (90-100 ºC), 5 ml of sodium citrate (38.8 mM) were added rapidly in continuous mode to the 50 ml of $HAuCl_4.3H_2O$ solution. The solution was kept in reflux for 1 hour. A color change was observed within the first minutes from pale yellow, through colorless to black and finally to a wine-red colored solution, indicating the formation of AuNPs. After 1 hour of heating the hot plate was switched off and the solution was left for cooling at room temperature with continuous agitation.

AgNPs were prepared by using a chemical reduction method. Distilled water was used to prepare all reacting solutions. For this synthesis, a 2-neck round-bottom flask

containing a solution of 50 ml of the aqueous $AgNO_3$ (1×10^{-3} M) was placed on the top of a heater plate and heated up to boiling temperature. As soon as the solution commenced to boil, 1 ml of sodium citrate solution (1%) was added drop by drop to the $AgNO_3$ solution. Vigorous stirring and boiling of the solution were kept during the whole process. The colour of the solution slowly turned into greyish yellow, indicating the reduction of the Ag^+ ions and so the formation of AgNPs. The reaction solution was maintained in reflux with vigorous mechanical stirring for 45 minutes and was later left to cool down to room temperature with continuous stirring.

5.5. Seed-mediated growth of AuNPs

Seed particle solutions were prepared according to the standard citrate reduction method. Firstly, 1.25 ml of a 10 mM $HAuCl_4.3H_2O$ solution (0.2% w/v) in 50 ml of deionized water was heated to boiling. At the same time, a solution of sodium citrate (1% w/v) containing citric acid (0.05% w/v) was prepared in 20 ml of deionized water. Then 2 ml of the sodium citrate containing citric acid solution were added quickly under vigorous stirring. The solution was kept in boiling for 5 minutes and was then allowed to cool down for 30 minutes. The colour of the mixed solution changed to wine red in several minutes, indicating the formation of AuNPs.

For the first growth step, 3 ml of the prior resulting seed solution were diluted to 20 ml and placed into a 3-neck bottom flask. Another two solutions were additionally prepared: one solution was prepared by diluting 2.25 ml of $HAuCl_4.3H_2O$ (10 mM) to 25 ml of deionized water and the other one was prepared by diluting a mixture of 1.25 ml of ascorbic acid solution (1%) and 0.625 ml of sodium citrate (1%) again to 25 ml. A 10 ml aliquot of the aforementioned solution containing $HAuCl_4.3H_2O$ (0.9 mM) and 10 ml of the aforementioned reducing solution containing sodium citrate and ascorbic acid were added separately to the 3-neck bottom flask at room temperature through Teflon tubes via a peristaltic pump under vigorous stirring over a time of about 42 minutes. After the addition was complete the mixture was brought to boiling for about 30 minutes.

For the second growth step, 4.5 ml of the resulting seed solution were diluted in 20 ml and placed again into a new and washed 3-neck bottom flask. Similarly, a 10 ml aliquot of the solution containing $HAuCl_4.3H_2O$ (0.9 mM) and 10 ml of the solution containing sodium citrate (1%) and ascorbic acid (1%) were added separately to the 3-neck bottom flask. The mixture was then brought to boiling for about 30 minutes and allowed to cool down.

5.6. Filtration of cardiac troponin I (Removal of 2-mercaptoethanol)

100 µl of a buffer solution were added to the centrifugal filter containing 100 µl of protein. The solution was then put to centrifuge. Centrifugations were carried out at 12.000 g for 20 minutes. Cardiac troponin I was diluted until a final concentration of 5×10^{-3}mM (Figure 38).

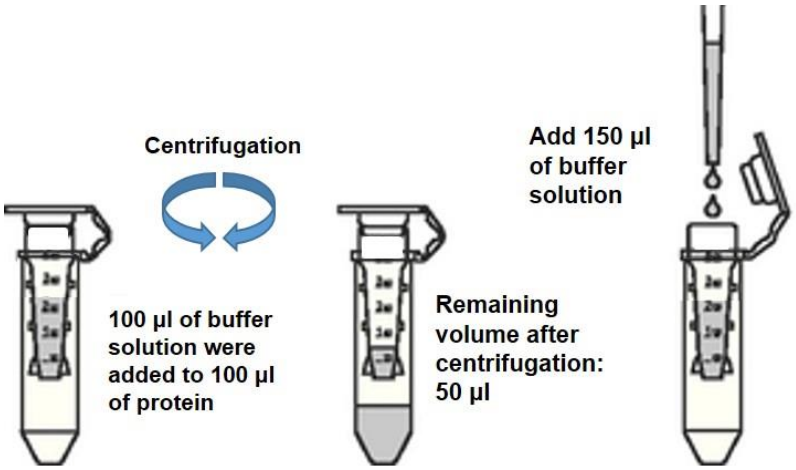

Figure 38. Illustration of the filtration of cardiac troponin I.

5.7. Buffer solution preparation

The buffer solution (pH=9.2) used for stabilization and preservation of the filtered cardiac troponin I was composed by 500 mM of sodium chloride (Nacl), 40 mM of TRIS ($C_4H_{11}NO_3$), 4mM of magnesium chloride ($Mgcl_2$) and 4 mM of calcium chloride ($Cacl_2$).

5.8. Preparation of samples for SERS assays

Samples for SERS measurements were prepared by adding 10 µl (5×10^{-3} mM) of human cardiac troponin I to 990 µl of colloids. Magnesium chloride ($Mgcl_2$) was added to the colloid to induce aggregation.

5.9. References

[1] Owen, T., *Fundamentals of UV-Vis spectroscopy,* 1996.

[2] Stiufiuc, R., lacovita, C., Lucaciu, C., Stiufiuc, G.*, et al.*, "SERS-active silver colloids prepared by reduction of silver nitrate with short-chain polyethylene glycol", *Nanoscale Research Letters,* vol. 8, pp. 1-5, 2013.

[3] Lungu, M., Enescu, E., Grigore, F., Buruntia, N.*, et al.*, "Chemical preparation and properties of some high concentrated colloidal silver solutions for antimicrobial applications", *Revue Roumaine de Chimie,* vol. 57, pp. 849-855, 2012.

[4] Erickson, D., Li, D., and Werner, C., "An Improved Method of Determining the zeta-Potential and Surface Conductance", *Journal Colloid and Interface Science,* vol. 232, pp. 186-197, 2000.

[5] http://www.silver-colloids.com/Tutorials/Intro/pcs17.html (22-07-2014).

[6] Zhang, Y., Yang, M., Portney, N. G., Cui, D.*, et al.*, "Zeta potential: a surface electrical characteristic to probe the interaction of nanoparticles with normal and cancer human breast epithelial cells", *Biomedical Microdevices,* vol. 10, pp. 321-8, 2008.

[7] Luque, R. and Varma, R. S., *Sustainable preparation of metal nanoparticles*, 2013.

[8] Stuart, B., *Infrared Fundamentals and Applications*, 2004.